SEPTEMBER 2021 M.Sc. in Aircraft and Aerospace Engineering KUTAIBA SROUR

REPUBLIC OF TURKEY

GAZİANTEP UNIVERSITY

GRADUATE SCHOOL OF NATURAL & APPLIED SCIENCES

A 6DOF NONLINEAR SIMULATION OF A SATELLITE MISSILE

M.Sc. THESIS

IN

AIRCRAFT AND AEROSPACE ENGINEERING

BY

KUTAIBAH SROUR

SEPTEMBER 2021

A 6DOF NONLINEAR SIMULATION OF A SATELLITE MISSILE

M.Sc. Thesis

In

Aircraft and Aerospace Engineering

Gaziantep University

Supervisor

Assist. Prof. Dr. Sohayb ABDULKERIM

by

Kutaibah SROUR

September 2021

SIMULATION OF A 6DOF NONLINEAR SATELLITE MISSILE

Submitted by **Kutaibah SROUR** in partial fulfillment of the requirements for the degree of Master of Science in **Aircraft and Aerospace Engineering**, **Gaziantep University** is approved by,

Prof. Dr. Mehmet İshak YÜCE
Director of the Graduate School of Natural and Applied Sciences .....

Assoc. Prof. Dr. İbrahim GÖV
Head of the Department of Aircraft and Aerospace Engineering .....

Asst. Prof. Dr. Sohayb ABDULKERİM
Supervisor, Aircraft and Aerospace Engineering
Gaziantep University .....

Graduation Date: 20. September. 2021

Examining Committee Members:

Asst. Prof. Dr. Sohayb ABDULKARIM
Aircraft and Aerospace Engineering
Gaziantep University .....

Asst. Prof. Dr. Dia Eddin NASSANI
Civil Engineering
Hasan Kalyoncu University .....

Assoc. Prof. Dr. Eyüp YETER
Aircraft and Aerospace Engineering
Gaziantep University .....

I hereby declare that all information in this document has been obtained and presented in accordance with academic rules and ethical conduct. I also declare that, as required by these rules and conduct, I have fully cited and referenced all material and results that are not original to this work.

Kutaibah SROUR

ABSTRACT

A 6DOF NONLINEAR SIMULATION OF A SATELLITE MISSILE

SROUR, Kutaibah
M.Sc. Aircraft and Aerospace Engineering
Supervisor: Assoc. Prof. Dr. Sohayb ABDULKERIM
September 2021
79 pages

Recently, it has been witnessed a significant increase in the number of controlled missiles for various purposes specifically for launching satellites. To validate the performance of an air vehicle, and to carry out the designing process of the controller and stabilizer, missiles need to be perfectly modeled and simulated. The literature is very meager in the simulation of missiles using 6DOF model. Therefore, this project simulates the missile using 6DOF by SIMULINK. To perform the simulation, dynamical equations using newton's second law were derived. The resulted dynamical equations, a set of nonlinear time-variant and coupled differential equations, were simulated using MATLAB without the need for a linearization process. The thrust vector and inertia tensor were defined using tabular data which functions on time, while the aerodynamics and stability derivatives were also determined by tables that function to Mach's number, angle of attack, and slide slip angles. The simulation process was validated by comparing the resulted trajectory for a case study with a similar one found in the literature. The comparison showed a good agreement. The resulted simulator allowed to design and tuning of PID controller using the Ziegler-Nichols method. This approach showed high flexibility and efficiency in finding missile trajectory and designing controller and stabilizer.

Key Words: Simulation, Missile, 6DOF, Trajectory, PID.

ÖZET

6DOF DOĞRUSAL OLMAYAN UYDU FÜZESİ SİMÜLASYONU

SROUR, Kutaibah
Yüksek Lisans Tezi, Uçak ve Uzay Mühendisliği
Danışman: Doç. Dr. Sohayb ABDULKERIM
Eylül 2021
79 sayfa

Son zamanlarda, çeşitli amaçlar ve özellikle uydu fırlatma amaçlı, kontrollü füzelerin sayısında önemli bir artışa tanık olunmaktadır. Bir hava aracının performansını doğrulamak, kontrolör ve dengeleyicinin tasarım sürecini gerçekleştirmek için füzelerin doğru bir şekilde modellenmesi ve simüle edilmesi gerekir. 6DOF modelini kullanan füzelerin simülasyonunda literatür çok yetersizdir. Bu nedenle, bu proje füzeyi SIMULINK tarafından 6DOF kullanarak simüle eder. Simülasyonu gerçekleştirmek için Newton'un ikinci yasasını kullanarak dinamik denklemler türetilmiş ve ardından MATLAB kullanılarak, terim terim simüle edilmiştir. Ortaya çıkan dinamik denklemler, doğrusal olmayan, zamanla değişmeyen ve birleştirilmiş diferansiyel denklemler kümesiydi. Füze itme ve atalet tensörü, zamanın fonksiyonu olan tablo verileri kullanılarak tanımlanırken, aerodinamik ve stabilite türevleri de Mach sayısı, saldırı açısı ve kayma kayma açılarına göre çalışan tablolarla belirlendi. Simülasyon süreci, bir vaka çalışması için elde edilen yörüngenin literatürde bulunan benzer bir yol ile karşılaştırılmasıyla doğrulanmıştır. Karşılaştırma, iyi bir uyuşma gösterdi. Ortaya çıkan simülatör, Ziegler-Nichols yöntemini kullanarak bir PID denetleyicisinin tasarlanmasına ve ayarlanmasına imkan verdi. Bu yaklaşım, füze yörüngesini bulma, kontrolör ve dengeleyici tasarlamada yüksek esneklik ve verimlilik gösterdi.

Anahtar Kelimeler: SIMULINK, Füze, 6DOF, Yörünge, PID.

''Dedicated to my family''

ACKNOWLEDGEMENTS

I would like to thank my supervisor, Assist. Prof. Dr. Sohayb ABDULKERIM for his guidance and support throughout the study. I am thankful for his encouragement and motivation.

I would like to express my love and gratitude to my family for their support, always best wishes.

TABLE OF CONTENTS

LIST OF TABLES

LIST OF FIGURES

LIST OF SYMBOLS

$\mathbf{F}$	force acting on a particular body, N
$\mathbf{M}$	moment acting on a particular body, N
$\mathbf{m}$	mass of a particle or body, Kg
$\mathbf{A}$	translational acceleration, m/s^2
$\mathbf{I}$	moment of inertia of a body, $kg.m^2$
$\dot{\boldsymbol{\omega}}$	angular acceleration, rad/s^2
$\mathbf{C}_{\boldsymbol{F}}$	general aerodynamic force coefficient, dimensionless
$\mathbf{C}_{\boldsymbol{M}}$	general aerodynamic moment coefficient, dimensionless
$\mathbf{d}$	aerodynamic reference length of body, m
$\mathbf{F}_{\boldsymbol{A}}$	aerodynamic force acting on a particular body, N
$\mathbf{M}_{\boldsymbol{A}}$	aerodynamic moment acting on a particular body, N.m
$\mathbf{P}_{\boldsymbol{a}}$	atmospheric pressure, pa
$\boldsymbol{\rho}$	atmospheric density, kg/m^3.
$\left(\frac{d\boldsymbol{\beta}}{dt}\right)_{inert}$	time rate of change of B relative to inertial frame
$\left(\frac{d\boldsymbol{\beta}}{dt}\right)_{rot}$	time rate of change of $\boldsymbol{B}$ relative to rotating frame
$\boldsymbol{\omega}$	angular rate vector of rotating frame relative to inertial frame, $rad/s\left(\text{deg}/s\right)$
$\boldsymbol{V}$	absolute linear velocity vector of a body
$\boldsymbol{A_e}$	rocket nozzle exit area, m^2
$\boldsymbol{F_p}$	total instantaneous thrust force vector, N
$\dot{\mathbf{m}}_{\mathbf{e}}$	mass rate of flow of exhaust gas, $\left(\dot{m}_e = -\dot{m}\right)$, kg/s

$\mathbf{P}_e$	average pressure across rocket nozzle exit area, pa
$\mathbf{t}$	time, s
$\dot{V}$	absolute acceleration vector of center of mass of missile, m/s^2
$\mathbf{F}_A$	resultant aerodynamic force vector,
$\mathbf{F}_g$	gravitational force vector including effects of earth rotation, N
$\mathbf{i}_b, \mathbf{j}_b, \mathbf{k}_b$	unit directions of xb-, yb-,and zb-axes (body coordinate system), respectively, dimensionless
$\mathbf{p}, \mathbf{q}, \mathbf{r}$	components of the angular rate vector expressed in body coordinate system (roll, pitch, yaw, respectively), rad/s
$u, \mathbf{v}, \mathbf{w}$	components of absolute linear velocity vector $\mathbf{V}$ expressed in body coordinate system m/s
$\mathbf{F}_{x_b}, \mathbf{F}_{y_b}, \mathbf{F}_{z_b}$	components of total force vector F expressed in the body coordinate system, N
$\dot{u}, \dot{\mathbf{v}}, \dot{\mathbf{w}}$	components of linear (translational) acceleration expressed in body coordinate system, m/s^2
$x, \mathbf{y}, \mathbf{z}$	coordinates of infinitesimal masses of the body, $\mathbf{m}$ & dm= infinitesimal mass, kg.
$\dot{\mathbf{h}}_{\mathbf{rot}}$	magnitude of the rate-of-change vector angular momentum h relative to (as viewed by an observer in) a rotating reference frame, N.m
$\mathbf{C}_D$	aerodynamic drag coefficient, dimensionless
$\mathbf{C}_\mathbf{L}$	aerodynamic lift coefficient, dimensionless
$\mathbf{C}_l$	aerodynamic roll moment coefficient about center of mass, dimensionless
$\mathbf{C}_m$	aerodynamic pitch moment coefficient about center of mass, dimensionless
$\mathbf{C}_n$	aerodynamic yaw moment coefficient about center of mass, dimensionless

$\dot{p}, \dot{q}, \dot{r}$	components of angular acceleration w expressed in body coordinate system (roll, pitch, and yaw, respectively), rad/s^2
I_x, I_y, I_z	moments of inertia (diagonal elements of inertia matrix when products of inertia are zero), Kg.m^2
L_A, M_A, N_A	components of aerodynamic moment vector M_A expressed in body coordinate system (roll, pitch, and yaw, respectively, N.m.
L_p, M_p, N_p	components of propulsion moment vector expressed in body coordinate system (roll, pitch, and yaw, respectively, N.m
A	magnitude of aerodynamic axial force vector, N
D	magnitude of aerodynamic drag force vector, N
L	magnitude of aerodynamic lift force vector, N
N	magnitude of aerodynamic normal force vector, N
S	aerodynamic reference area, m^2
C_{D_0}	zero-lift drag coefficient dimensionless
C_{L_α}	slope of curve formed by lift coefficient C_L versus angle of attack a, $rad^{-1}(dag^{-1})$
C_{L_p}	roll damping derivative, $rad^{-1}(dag^{-1})$
K	constant depending on body shape and flow regime, dimensionless
C_{l_δ}	slope of curve formed by roll moment coefficient Cl versus control-surface deflection, δr. $rad^{-1}(dag^{-1})$
α	angle of attack in pitch plane, rad (deg)
$\delta_r, \delta_p, \delta_y$	angles of effective control surface deflections in (roll, pitch, yaw)directions
$F_{A_{yb}}$	y_b -component of aerodynamic force in body coordinate system, N.
$F_{A_{xb}}$	z_b -component of aerodynamic force in body coordinate system, N.

$\mathbf{M_N}$	Mach number, dimensionless.
$\mathbf{C_{mref}}$	pitching moment coefficient about reference moment station, dimensionless
$\mathbf{C_{nref}}$	yawing moment coefficient about reference moment station, dimensionless
$\boldsymbol{\beta}$	angle of sideslip (angle of attack in yaw plane), rad (deg)
$\mathbf{C_{ny}}$	coefficient corresponding to component of normal force on y_b-axis, dimensionless
$\mathbf{C_{nz}}$	coefficient corresponding to component of normal force on z_b-axis, dimensionless
$\mathbf{C_{nr}}$	yaw damping derivative relative to yaw rate r, $rad^{-1}\left(\deg^{-1}\right)$
$\mathbf{C_{n\beta}}$	slope of curve formed by yawing moment coefficient C_n versus angle of sideslip β, $rad^{-1}\left(\deg^{-1}\right)$
$\mathbf{C_{n\delta}}$	slope of curve i.e yawing moment coefficient C_n versus control-surface deflection δ_y. $rad^{-1}\left(\deg^{-1}\right)$
$\mathbf{C_{m\alpha}}$	slope of curve formed by pitch moment coefficient C_m versus angle of attack α, $rad^{-1}\left(\deg^{-1}\right)$
$\mathbf{C_{m\delta}}$	slope of curve i.e. pitch moment coefficient C_m versus control-surface deflection δ_p. $rad^{-1}\left(\deg^{-1}\right)$
$\boldsymbol{Q}$	dynamic pressure parameter, P_a
$\boldsymbol{a}$	lapse rate, k/m
$\mathbf{g_0}$	magnitude of the acceleration vector $\vec{g}_0$ due to gravity at the earth surface, m/s^2

$\boldsymbol{h}$	altitude for which atmospheric properties are to be calculated above sea level, m
$\mathbf{h_1}$	reference altitude (e.g., sea level or earth surface), m
$\boldsymbol{p}$	pressure at altitude h, P_a
$\mathbf{p_1}$	given pressure at altitude h1, P_a
$\boldsymbol{R}$	gas constant (287.05), N.m/(Kg.k)
$\boldsymbol{T}$	temperature at altitude h, k
$\mathbf{T_1}$	given temperature at altitude h1, k
$\mathbf{V_s}$	speed of sound at altitude h, m/s
$\boldsymbol{\delta}$	ratio of specific heat, dimensionless
$\mathbf{F_P}$	magnitude of instantaneous thrust force, N
$\mathbf{F}_{p_{xb}}, \mathbf{F}_{p_{yb}}, \mathbf{F}_{p_{zb}},$	components of thrust vector $\mathbf{F}\boldsymbol{p}$ expressed in the body coordinate system, N
$\boldsymbol{m(t)}$	instantaneous mass of missile, kg.
$\mathbf{m_0}$	missile mass of the missile at time zero (i.e.,at the time of launch), kg
$\mathbf{m}_{b0}$	missile mass of the missile at burnout, kg
$\mathbf{F}_p(t)$	instantaneous input thrust produced by missile engine (at different altitudes), N
$\mathbf{F}_{pref}$	reference thrust force (tabulated values), N
$\mathbf{I}_{sp}$	specific impulse of propellant, N.s/Kg
$\mathbf{X}_{cm}(t)$	instantaneous distance from missile noze to center of mass,
$\mathbf{X}_{cm0}$	distance from missile noze to center of mass at launch,
$\mathbf{X}_{cmb0}$	distance from missile noze to center of mass at burnout,
$\mathbf{I}(t)$	instantaneous moment of inertia,kg. m^2
$\mathbf{I_0}$	moment of inertia at launch,. m^2
$\mathbf{I}_{b0}$	moment of inertia at burnout,. m^2

$\mathbf{F}_{g_{xe}}, \mathbf{F}_{g_{ye}}, \mathbf{F}_{g_{ze}}$	components of gravitational force vector $\vec{F}_g$ expressed in the earth coordinate system
g	magnitude of acceleration-due-to-gravity vector $\vec{g}, m/s^2$
θ	Euler angle rotation in elevation (pitch angle), rad(deg)
ϕ	Euler angle rotation in roll (roll angle), rad(deg)
ψ	Euler angle rotation in yaw (yaw angle), rad(deg)
$\dot{\theta}, \dot{\psi}, \dot{\phi}$	rates of change of Euler angles in heading, pitch, and roll, respectively, rad/s (deg/s)

LIST OFABBREVIATIONS

EOM	Equation of Motion
DTR	Degree to Radian
RTD	Radian to Degree
IC	Initial Condition
DOF	Degree of Freedom
PID	Proportional, Integral, Differential
DCM	Direction Cosine Matrix

CHAPTER I

INTRODUCTION

1.1 Introduction

The designing process of a missile control system is normally performed through several phases. The first phase is started by deriving the equation of motion which is, in general, nonlinear and coupled, then solving the resulted equations using various methods, which allows obtaining the 3D position, the 3D orientation of the missile, the velocity components, roll, pitch, and yaw rate, angle of Attack, sideslip angle, and Euler angles. The second phase : the set of differential equations are linearized about particular flight conditions allowing to derive the transfer functions of the dynamical system which allows to analyze the stability and to find the stabilizer and the appropriate controller for a certain task (AKSu, 2013), (Bhagwandin & Sahu, 2012)(Shelton et al., 2018).

This thesis focused on the first phase and the development of a MATLAB program suitable for general missile giving the aerodynamics and stability derivatives $C_{D0}, C_{L\alpha}, C_{m\alpha}, C_{m\delta}, C_{n\beta}, C_{n\delta}, C_{mq}+C_{m\dot{\alpha}}, C_{nr}+C_{n\dot{\beta}}, K$, in addition to damping coefficients $C_{mq}+C_{m\dot{\alpha}}$, $C_{nr}+C_{n\dot{\beta}}$ these coefficients have a profound effects on the dynamical behavior hence on the designing process of the missile control (R. D. Finck, 1978). These coefficients are normally found using serval methods, to mention a few, MISSILE-DATCOM software, the Semi empirical- based code, is used to predict those coefficients, in the last double decades, due to the huge development in the computation capabilities, CFD packages have been emerged which are capable of estimating the aerodynamics characteristics accurately (Oktay & Akay, 2002). Reportedly, CFD methods showed good agreements with experimental and/or the Semi empirical method (Stalnaker & Robinson, 2002)(R. D. Finck, 1978).

after obtaining the aerodynamic coefficients by using one of the method that mentioned above, the equation of motion can be found and then solving it by using

MATLAB software, then it can be used by the system identification method to derive the linear mathematical model (Kisabo et al., 2019) or we can use the nonlinear model directly (Kisabo et al., 2019) and control it using PID controller.

In this work, a set of aerodynamics coefficients for a particular case, found in the literature, were used for a detailed case study. The resulted trajectory of the simulation process was plotted and compared for the same case study. It was found some acceptable agreements giving the verification for the in-house developed code. Then the same code was used to tune the PID controller using Ziegler–Nichols method.

The thesis is describing the work in 9 chapters. The first chapter includes the general introduction which reviews the steps that were followed to simulate and control the general missiles. Chapters 2, 3, and 4 give a theoretical background for the missile simulation process. Chapter 5 includes the demonstration of simulation blocks for every equation of the set of the EOM. Chapter 6 reviews the Zieger-Necholas method and explains how it was used to design the stabilizer. Chapter 7 explores the validation of the simulation approach. Chapter 8 includes the simulation scenario for surface to air missile targeting a flying object. Chapter 9 includes the recommendation and the conclusions.

CHAPTER II

DYNAMIC MODELING OF MISSILES

2.1 Description of a Missile Flight Simulation

Missile flight modeling is a computer program that calculates the missile's trajectory and other vital parameters as it leaves the launcher. a mathematical model of the missile and its surroundings are used in the simulation. Equations which describe physics rules and logical sequences make up these mathematical models. The missile model includes information about the missile's mass, propulsion aerodynamics, navigation system, as well as the equations needed to compute the missile's orientation and trajectory as well as the equations required to determine the missile's orientation and trajectory. At the very least, the atmospheric property and gravity effect are included in the environmental model. Other elements, such as fog, haze, sun position, terrain, and/or sea level features, could be incorporated if they have a significant impact on the simulation's goals. To replace t, breadboard components or actual missile hardware could be employed. (Belkacem & Bachir, 2019).

In simulation, the rules of physics are the rules that determine missile motion and the laws that impact the simulated component. The equation of motion for the missile, for example, determines the acceleration, velocity, and position caused by the forces of gravity, thrust, and aerodynamics. Figure 2.1 depicts the missile flight simulator's inputs and outputs. The data required for a mathematical equation is known as (input), and it can be transferred from one device to another.

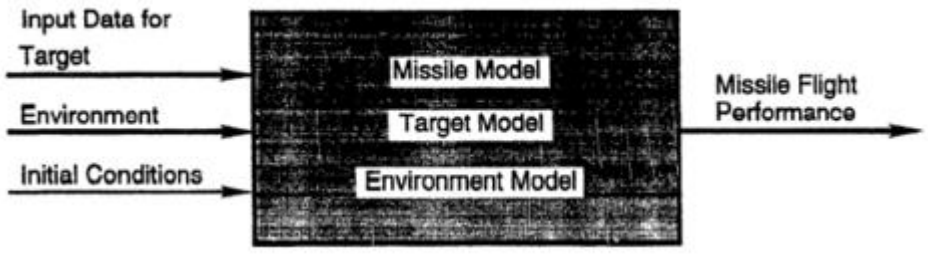

Figure 2.1 Missile Flight (Belkacem & Bachir, 2019).

2.2 Simulation of Missile Motion

Physical principles are used to create computer models that simulate missile movement: the use of propulsion, aerodynamic force, and gravity, as well as each missile's response to these forces. Newton's second law is used to model missile motion mathematically. At any given time, the force exerted on the rigid body accelerates the body's center of gravity. Force is directly proportional to acceleration. The reciprocal of the body's mass is the proportionality constant. It is a pure translational movement when the force vector crosses through the center of gravity. The immediate rotational acceleration of the transition combination object is related to the moment of force operating around the axis via the center of gravity if the force vector does not cross through the center of gravity. The reciprocal of the object's moment of inertia around its axis is the constant of proportionality in this situation. These ideas are stated mathematically as well-known equations.

$$F = ma \tag{2.1}$$

$$M = I\dot{\omega} \tag{2.2}$$

Almost every flight simulation includes three primary factors acting on a missile: gravity, propulsion, and aerodynamics.

2.3 Missile Dynamics

The mathematical formulas employed in the missile flight simulation model describe the dynamic movement of the missile generated by forces and moments operating on it. The equation of motion is a mathematical tool that describes the link between forces acting on a missile and the missile's movement as a result of those forces .Understanding these mathematical correlations is the goal of analyzing missile dynamics in flight simulation. The translational equation of motion is applied to the three-degree-of-freedom model. The rotating equation of motion is used in the 6DOF model as well. Forces and moments operating on the missile are used as inputs to the equation of motion. Forces and moments produce the output, which is the missile's acceleration.

Aerodynamics, propulsion, and gravity all produce forces and moments. Aerodynamic forces and moments are created when air flows over a missile. They are determined by the speed, composition, and orientation of the missile, as well as the properties of the surrounding air. Typically, the thrust is designed to operate on the missile's center of

gravity, resulting in no moment surrounding the center of gravity. The equation of motion is founded on Newton's law of motion and is only applicable to reference frames that are not accelerated. However, stating it in the context of a rotating body substantially simplifies the calculation of a spinning missile's movement. To adapt Newton's law to the rotational coordinate system, the equation of motion must be adjusted.

Generally, a missile's forces and moments are decomposed into elements in the body coordinate frame or the wind coordinate frame. The use of the body's coordinate frame to match the body's axis of rotation with the coordinate system's axis is emphasized in this study. a mathematical program is required to convert the rate of change vector to a vector related to the inertial frame as shown in Figure 2.2. The following is the general formula for calculating the rate of change of the vector in the inertial frame:

$$\left(\frac{dB}{dt}\right)_{inert} = \left(\frac{dB}{dt}\right)_{rot} + (\omega \times B) \tag{2.3}$$

2.3.1 Translational Equations

The common approach for solving the translational equation of motion in missile flight simulations is to calculate the total of forces using aerodynamic, propulsive, and gravitational data, then changing the substitution with the equation of motion and calculating the actual acceleration.

$$\left(\dot{V}_{x_b}\right)_{inrt} = \frac{F_{x_b}}{m} \tag{2.4}$$

$$\left(\dot{V}_{y_b}\right)_{inrt} = \frac{F_{y_b}}{m} \tag{2.5}$$

$$\left(\dot{V}_{z_b}\right)_{inrt} = \frac{F_{z_b}}{m} \tag{2.6}$$

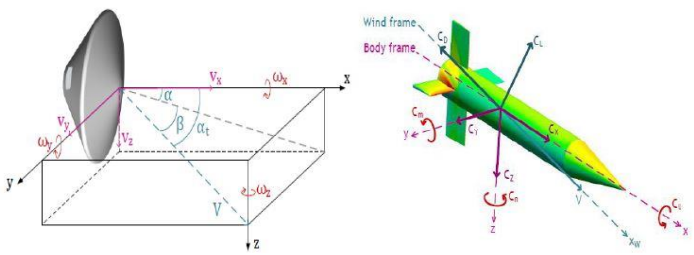

Figure 2.2 Missile Axis (Belkacem & Bachir, 2019).

The vectors $\boldsymbol{\omega}$ and **V** are expressed as:

$$\omega = pi_b + qj_b + rk_b \tag{2.7}$$

$$V = ui_b + vj_b + wk_b \tag{2.8}$$

and the cross product is given as

$$\omega \times v = (q\omega - rv)i_b + (ru - pw)\,j_b + (pv - qu)k_b \tag{2.9}$$

We know that $\dot{V}_{rot} = \dot{V}_{inrt} - (\omega \times v)$ which implies that

$$\dot{u} = \frac{F_{x_b}}{m} - (qw - rv) \tag{2.10}$$

$$\dot{v} = \frac{F_{y_b}}{m}(ru - pw) \tag{2.11}$$

$$\dot{w} = \frac{F_{z_b}}{m} - (pv - qu) \tag{2.12}$$

Similar symbols, represented by the subscripts *y* and z, represent the components of the total force *y* and *z*, respectively. afterwards

$$\dot{u} = \frac{F_{A_{x_b}} + F_{p_{x_b}} + F_{g_{x_b}}}{m} - (qw - rv) \tag{2.13}$$

$$\dot{v} = \frac{F_{A_{y_b}} + F_{p_{y_b}} + F_{g_{y_b}}}{m}(ru - pw) \tag{2.14}$$

$$\dot{w} = \frac{F_{A_{z_b}} + F_{p_{z_b}} + F_{g_{z_b}}}{m} - (pv - qu) \tag{2.15}$$

2.3.2 Rotational Equations

Moments acting on the missile are derivative of angular momentum that is used to compute the missile's angular velocity. (Belkacem & Bachir, 2019). In the angular momentum vector h, the angular velocity is taken into account. In most cases, the relationship with h includes an inertial matrix if the rotation axis is unbound. (Also known as an inertia tensor) [***I***]. This relationship is caused by

$$[I] = \begin{bmatrix} I_{xx} & -I_{xy} & -I_{xz} \\ -I_{xy} & I_{yy} & -I_{yz} \\ I_{xz} & I_{yz} & I_{zz} \end{bmatrix} \tag{2.16}$$

$$I_{\chi\chi} = \int \left(y^2 + z^2 \right) dm \tag{2.17}$$

$$I_{\chi y} = \int \left(xy \right) dm \tag{2.18}$$

$$I_{yy} = \int \left(\chi^2 + z^2 \right) dm \tag{2.19}$$

$$I_{xz} = \int \left(xz \right) dm \tag{2.20}$$

$$I_{zz} = \int \left(y^2 + x^2 \right) dm \tag{2.21}$$

$$I_{zz} = \int \left(yz \right) dm \tag{2.22}$$

The reference frame axis, where the inertial product term disappears, is always selectable for a particular direction of the body, so:

$$[I] = \begin{bmatrix} I_{xx} & 0 & 0 \\ 0 & I_{yy} & 0 \\ 0 & 0 & I_{zz} \end{bmatrix} \tag{2.23}$$

Since the angular momentum h is a vector, the rate of change with time in the inertial coordinate system differs from the rate of change in the rotational coordinate system. (Cover, 1995). Again, take this difference into account

$$M = \dot{h}_{rot} + \omega \times h \tag{2.24}$$

$$\dot{h}_{rot} = [I]\dot{\omega} \tag{2.25}$$

$$\omega \times h = qr(I_z - I_y)i_b + pr(I_x - I_z)j_b + pq(I_y - I_x)k_b \tag{2.26}$$

This leads to the following rotation equations

$$\dot{p} = [L - qr(I_z - I_y)] / I_x \tag{2.27}$$

$$\dot{q} = [M - pr(I_x - I_z)] / I_y \tag{2.28}$$

$$\dot{r} = [N - pq(I_y - I_x)] / I_z \tag{2.29}$$

The angular acceleration is calculated using these equations when the missile moment is supplied. When the moment term *L* is divided into an aerodynamic component and a propulsion component, the equation becomes as follow:

$$\dot{p} = [L_A + L_p - qr(I_z - I_y)] / I_x \tag{2.30}$$

$$\dot{q} = [M_A + M_p - pr(I_x - I_z)] / I_y \quad (2.31)$$

$$\dot{r} = [N_A + N_p - pq(I_y - I_x)] / I_z \quad (2.32)$$

2.4 Missile Aerodynamics

The equations for computing the aerodynamics forces and moments necessary as input parameters to the equation of motion are summarized here. Lift and angle of attack are assumed to be linear in the aerodynamic coefficient formula. The polarity of lift and drag is parabolic., as well as the torque coefficient is linear in relation to the variables that influence it. Further realistic nonlinear aerodynamic variables should be input into the simulation in tabular format if it is accessible and required for the simulation aim. Then look over the table and modify the equation for the aerodynamic coefficient. Instead, a non-linear term can be added to the equation presented here.

2.4.1 Aerodynamic Forces

It is required to provide the factors affecting aerodynamics and torque in an acceptable connection in order to employ test data and empirical methodologies in flight simulation. In the area of aerodynamics, the relationship is defined by a frequently used form of aerodynamic equation. (Belkacem & Bachir, 2019).

The formulas used to calculate these forces and moments affecting the missile are:

$$D = 0.5\rho V^2 C_D S \quad (2.33)$$

$$L = 0.5\rho V^2 C_L S \quad (2.34)$$

$$F_y = 0.5\rho V^2 C_y S \quad (2.35)$$

$$L_A = 0.5\rho V^2 C_l S d \quad (2.36)$$

$$M_A = 0.5\rho V^2 C_m S d \quad (2.37)$$

$$N_A = 0.5\rho V^2 C_n S d \quad (2.38)$$

For rolling missiles, the drag is the same, but the lift and lateral force are:

$$L = 0.5PV^2 \cos(\varnothing) C_{L_T} S \quad (2.39)$$

$$F_y = 0.5PV^2 \sin(\varnothing) C_{L_T} S \quad (2.40)$$

$$C_{L_T} = \sqrt{C^2{}_y + C^2{}_L} \tag{2.41}$$

The linearity of lift and angle of attack is assumed in the aerodynamic coefficient equation and parabolic. Polarity is matched by lift and drag; moreover, the moment coefficient is linear in relation to the many parameters that influence it.

$$C_D = C_{D_0} + KC^2{}_L \tag{2.42}$$

$$C_L = C_{L\alpha} a \tag{2.43}$$

$$C_l = C_{l_\delta} \delta_r + \frac{d}{2V}\left(C_{1_p} p\right) \tag{2.44}$$

So, the axial, normal & side forces are inferring from drag and lift as the following:

$$A = D_{\cos}\left(\alpha_t\right) - L_{\sin}\left(\alpha_t\right) \tag{2.45}$$

$$N = D_{\sin}\left(\alpha_t\right) + L_{\cos}\left(\alpha_t\right) \tag{2.46}$$

$$\cos\left(\alpha_t\right) = \cos\left(\alpha\right)\cos\left(\beta\right) \tag{2.47}$$

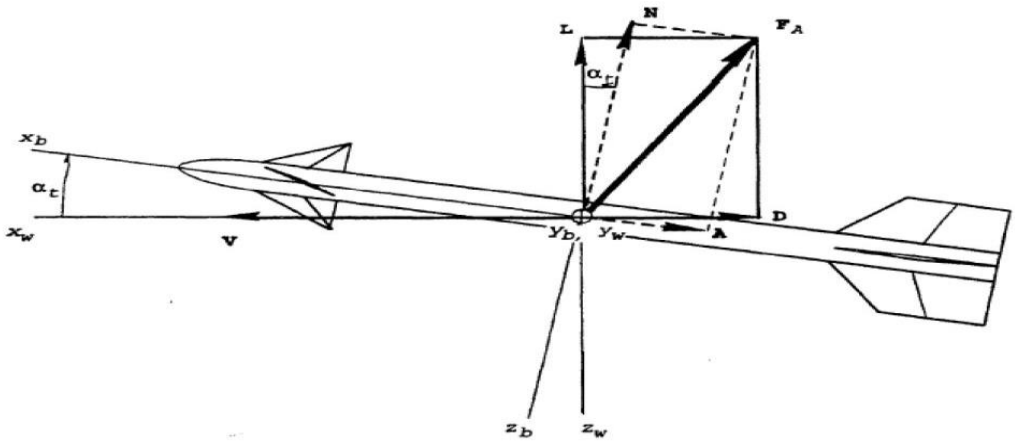

Figure 2.3 Missile Axial and Normal Force (Belkacem & Bachir, 2019).

Axial force ***A*** is directly opposite the xb-axis, $F_{A_{xb}} = -A$ as shown in Figure 2.3

It is possible to define the normal force vector in the coordinates of the body as follows:

$$F_{A_{y_b}} = N\left(\frac{-v}{\sqrt{v^2 + w^2}}\right) \tag{2.48}$$

$$F_{A_{z_b}} = N\left(\frac{-w}{\sqrt{v^2+w^2}}\right) \tag{2.49}$$

2.4.2 Moment Coefficients:

The moment that aerodynamic force exerts on the missile is calculated by the moment coefficients Cl, Cm and Cn, which are calculated from the roll angle, the pitch angle, and the yaw angle, respectively. a missile's moment coefficient is principally determined by its Mach number, angle of attack, and control surface displacement. The reference torque station is usually at the missile's center of gravity (CM or CG) after the motor burns out, however, before the engine runs out, the missile's center of gravity shifts over time owing to mass redistribution when the propellant has been burnt and discharged. As a result, the torque coefficient must be adjusted. The following are the formulas for calculating yaw and pitch moment coefficient corrections:

$$C_m = C_{m_{ref}} - C_{N_z}\left(\frac{x_{cm}-x_{ref}}{d}\right)+\frac{d}{2V}\left(C_{m_q}+C_{m_a}\right)q \tag{2.50}$$

$$C_n = C_{n_{ref}} + C_{N_y}\left(\frac{x_{cm}-x_{ref}}{d}\right)+\frac{d}{2V}\left(C_{n_r}+C_{n_\beta}\right)r \tag{2.51}$$

The pitch and yaw elements of the aerodynamic moment around the reference point are calculated using the formula below.

$$C_{m_{ref}} = C_{m_a}\alpha + C_{m_\delta}\delta_p \tag{2.52}$$

$$C_{n_{ref}} = C_{n_\beta}\beta + C_{\eta_\delta}\delta_y \tag{2.53}$$

Because the missile is supposed to have cruciform symmetry:

$$C_{n_\beta} = C_{m_a} \tag{2.54}$$

$$C_{n_\delta} = C_{m_\delta} \tag{2.55}$$

$$C_{n_r} = C_{m_q} \tag{2.56}$$

$$C_{n_{\dot\beta}} = C_{m_{\dot\alpha}} \tag{2.57}$$

In the y_b- and z_b-axes, coefficients relating to the components of the normal force are determined.

$$C_{N_y} = \frac{F_{A_{y_b}}}{QS} \tag{2.58}$$

$$C_{N_z} = \frac{F_{A_{z_b}}}{QS} \tag{2.59}$$

2.4.3 Aerodynamic Stability Derivatives:

Conceptual design and viability studies at an early stage of new missiles typically use estimated stability derivatives to generate aerodynamic coefficients before a large amount of aerodynamic data is acquired. However, it is advisable to use large amounts of tabular data directly after obtaining detailed aerodynamic data once the flight test data is obtained. Depending on the outcomes of flight tests, the aerodynamic coefficient parameters are fine-tuned. Estimates and measurements of such aerodynamic parameters are typically performed by the missile's engineer and then they are sent to the relevant government laboratory for analysis.

Note: there are many assumptions in the literature on aerodynamic data, but they are not always clearly expressed. Therefore, when using this information in missile simulations, more caution must be taken to verify its relevance. Here are a few "pitfalls" to stay away from:

- No set length or area for using it as a reference.
- Data relevant to Mach number-restricted regions .
- Data is only applicable to certain Reynolds number ranges.
- Data only applying to small angles of attack .
- Only one type of aerodynamic force is covered by the data.
- Data relevant for only two-dimensional flow .

2.5 Atmospheric Properties:

Aerodynamics is influenced by atmospheric conditions among other variables. Density is the most essential atmospheric variable used to determine the aerodynamics of incompressible fluid. It is required the ambient air sound speed to compute the aerodynamic force within compressible flow circumstances and to compute missile thrust as a result atmospheric pressure is needed. When the Reynolds number is taking as simulation parameter, the kinematic viscosity of the environment is required to compute it. Density fluctuates with atmospheric pressure, heat, speed of sound, but

viscosity only varies with temperature, according to the formula of air. For missile simulations, environmental data is normally given as a function of attitude in the style of tabular data. There are two fundamental ways in which the atmosphere impacts on missiles. For begin, the flow of the air on the missile's surface produces aerodynamic moment and force. Second, missile seekers' performance is influenced by the atmosphere's ability to transfer electromagnetic waves, so the pressure, density, and sound speed are the basic atmospheric parameters utilized in aerodynamic calculations.

During each calculation phase, an atmospheric database or model are used by a missile flight simulation to supply atmospheric parameters for the missile's actual altitude. (Belkacem & Bachir, 2019).

Flight simulations use a formula that extrapolates or interpolates the dataset based on established principles of atmospheric change with altitude in instances where observed atmospheric data is only available at one or a few heights as shown in Figure 2.4. These formulas are based on hydrostatic pressure concept, air state equations, and known atmospheric temperature behavior as a function of altitude. At an altitude of approximately 11,000 meters. Experiments show that at a maximum altitude of around 11,000 m, the temperature drops almost linearly with height. The troposphere is the name given to this region. The stratosphere is an isothermal area that extends from the troposphere to an altitude of roughly 21,000 m, where the temperature is nearly constant with respect to altitude.

The following simple assumptions are frequently employed in the equations used to estimate atmospheric properties:

- There is no moisture in the air.
- The air has the properties of a perfect gas.
- The gravitational field is always present.
- Within a certain altitude range, the rate of temperature change with height is constant.

$$T = T_1 + a\left(h - h_1\right) \tag{2.60}$$

$$P = P_1 + \left(\frac{T}{T_1}\right)^{\frac{g_0}{(aR)}} \tag{2.61}$$

$$\rho = \frac{p}{RT} \tag{2.62}$$

$$V_s = \sqrt{\gamma RT} \tag{2.63}$$

Within the troposphere, a typical lapse rate is 0.0065 K/m. The typical lapse rate is taken as zero in the stratosphere, and the pressure is substituted by:

$$P = P_1 \exp\left[-\frac{g_0}{RT}(h - h_1)\right] \tag{2.64}$$

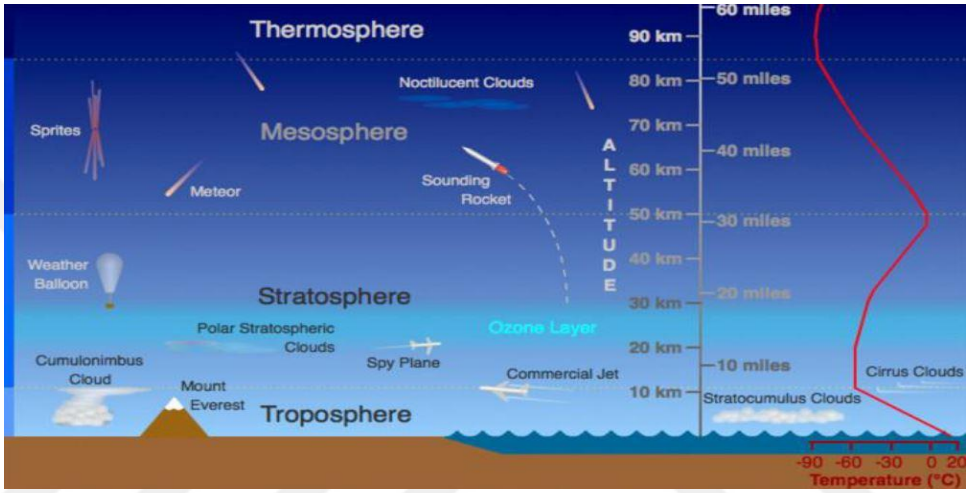

Figure 2.4 Atmosphere Properties with Altitude (Belkacem & Bachir, 2019).

2.6 Missile Propulsion

Liquid propellant rockets, air-enhanced rockets, turbojet engines, and ramjet engines are among several types of propellant motors used in missiles.
The amplitude of thrust FP in most missiles is directed along the xb-axis (the missile centerline). The following are the elements of the thrust vector FP represented in the body of reference coordinate system.

$$F_{p_{x_b}} = F_p \tag{2.65}$$

$$F_{p_{y_b}} = 0 \tag{2.66}$$

$$F_{p_{z_b}} = 0 \tag{2.67}$$

When the thrust is angled away from the missile's axis by $\gamma 1$ and $\gamma 2$, as shown in Figure 2.5, the thrust vector's elements are provided by:

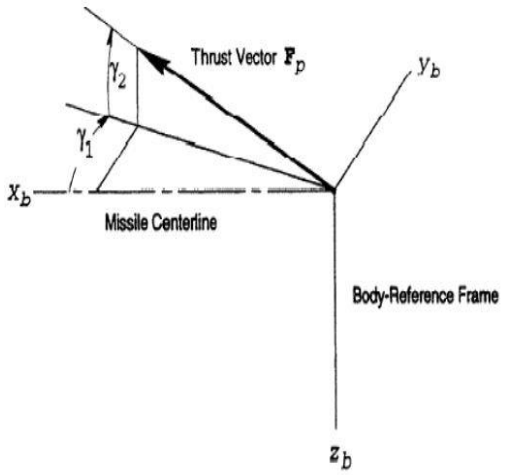

Figure 2.5 Missile Propulsion Misaligned from Missile Axis

$$F_{p_{x_b}} = F_p \cos\gamma_2 \cos\gamma_1 \tag{2.68}$$

$$F_{p_{x_b}} = F_p \cos\gamma_2 \sin\gamma_1 \tag{2.69}$$

$$F_{p_{z_b}} = -F_p \sin\gamma_2 \tag{2.70}$$

The following equation gives the elements of the moment vector M_P:

$$L_p = 0 \tag{2.71}$$

$$M_p = F_{p_{z_b}} l_p \tag{2.72}$$

$$N_p = -F_{p_{y_b}} l_p \tag{2.73}$$

2.7 Time varying parameters

The amount of missile mass m is derived using a lookup table as a consequence of simulation time. (*Military Handbook. Missile Flight Simulation. Part one. Surface-to-Air Missiles (z-Lib.Org).Pdf*, n.d.), or, alternatively, m can be determined inside the simulation., by using the following:

$$m = m_0 - \frac{1}{I_{sp}} \int_0^t F_{p_{ref}} \, d\,\mathrm{t} \tag{2.74}$$

The input thrust database is often used to calculate the thrust F_{pref} as a function of time for the reference air pressure. The thrust is adjusted to compensate for the atmospheric pressure Pa.

$$F_p = F_{p_{ref}} + \left(p_{ref} - p_a \right) A_e \tag{2.75}$$

The moment of inertia also is recalculated using the following formula:

$$I = I_0 - \left(I_0 - I_{b0} \right) \left(\frac{m_0 - m}{m_0 - m_{b0}} \right) \tag{2.76}$$

Furthermore, the location of the x_{cm} center of mass is adjusted utilizing:

$$x_{cm} = x_{cm0} - \left(x_{cm0} - x_{cm_{b0}} \right) \left(\frac{m_0 - m}{m_0 - m_{b0}} \right) \tag{2.77}$$

CHAPTER III

MISSILE MOTION

3.1 Missile Motion:

In the simulation, the missile movements are calculated by the equation of motion under effects of various forces acting on the air-vehicle such as gravity, aerodynamics and propulsion forces (Belkacem & Bachir, 2019). The time history of translation, rotation positions and speeds are generated by integrating the nonlinear equations of motion during the simulated flight. Depending on the purpose of the simulation, the equation can usually be simplified to calculate the movement of the target. Alternatively, the equation of motion can be simplified to calculate the missile movement.

In some cases, if aerodynamic data is given using inappropriate set of coordinate axis. It may be necessary to make the appropriate conversions to the utilized set of axes for lift, drag, normal, and axial forces. For example, in the early stages of developing the missile concept, if no a large number of aerodynamic coefficient tables, the facts that the missile concept can be used and the force coefficients are usually nearly linear.

The angle of attack and the sideslip angle are determined using the following formulas:

$$\alpha = \mathrm{Tan}^{-1}\left(\frac{w}{u}\right) \tag{3.1}$$

$$\beta = \sin^{-1}\left(\frac{v}{V_M}\right) \tag{3.2}$$

For computing the angle of sideslip, an alternative and frequently used equation is:

$$\beta = \sin^{-1}\left(\frac{v}{u}\right) \tag{3.3}$$

The amount of the thrust force F_P is computed using the following formula:

$$F_p = F_{p_{ref}} + \left(p_{ref} - p_a\right) A_e \tag{3.4}$$

The gravitational force expressed in earth coordinates is given by:

$$F_{g_{x_e}} = 0 \tag{3.5}$$

$$F_{g_{y_e}} = 0 \tag{3.6}$$

$$F_{g_{z_e}} = mg \tag{3.7}$$

To determine gravity represented in body coordinates, multiply the vector Fg by the DCM matrix, which translates the vector of the earth frame into the body frame.

$$\begin{bmatrix} F_{g_{x_b}} \\ F_{g_{y_b}} \\ F_{g_{z_b}} \end{bmatrix} = \begin{bmatrix} C_\theta C_\psi & C_\theta S_\psi & -S_\theta \\ S_\phi S_\theta C_\psi - C_\phi S_\psi & S_\phi S_\theta S_\psi + C_\phi C_\psi & S_\phi C_\theta \\ C_\phi S_\theta C_\psi + S_\phi S_\psi & C_\phi S_\theta S_\psi - S_\phi C_\psi & C_\phi C_\theta \end{bmatrix} \begin{bmatrix} 0 \\ 0 \\ mg \end{bmatrix} \tag{3.8}$$

$$\left(F_g\right)_b = \left[T_{b/e}\right]\left(F_g\right)_e \Leftrightarrow \left(F_g\right)_e = \left[T_{b/e}\right]^T \left(F_g\right)_b = \left[T_{e/b}\right]\left(F_g\right)_b \tag{3.9}$$

3.2 Euler Angles

Many simulation features require missile orientation (azimuth), such as angle of attack, guide gimbal angle, and warhead spray mode calculations. In a six-DOF simulation. By integrating the equations that determine Euler's angular velocity, the missile attitude can be derived immediately.

$$\dot{\phi} = p + \left(q\sin\left(\phi\right) + r\cos\left(\phi\right)\tan\left(\theta\right)\right) \tag{3.10}$$

$$\dot{\theta} = q\cos\left(\phi\right) - r\sin\left(\phi\right) \tag{3.11}$$

$$\dot{\psi} = p + \left(q\sin\left(\phi\right) + r\cos\left(\phi\right)\right)/\cos\left(\theta\right) \tag{3.12}$$

CHAPTER IV

MATLAB SIMULATION

4.1 the equation of motion simulation

In this part the equation of motion blocks for the (u, v, w, p, q, r, ϕ , θ , ψ) will be displayed.

The translational parameters of the motion is described using blocks diagrams as shown in Figure 4.1, Figure 4.2, and Figure 4.3.

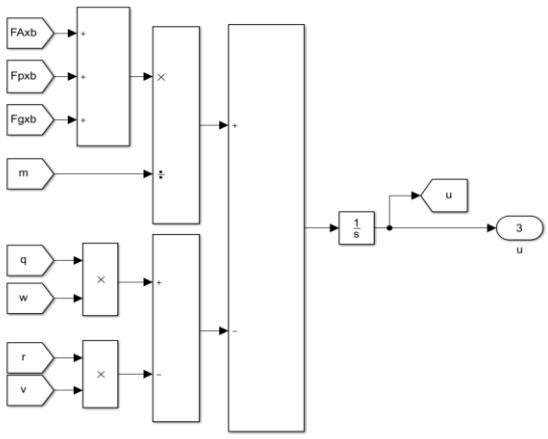

Figure 4.1 Simulation Block of u-Velocity

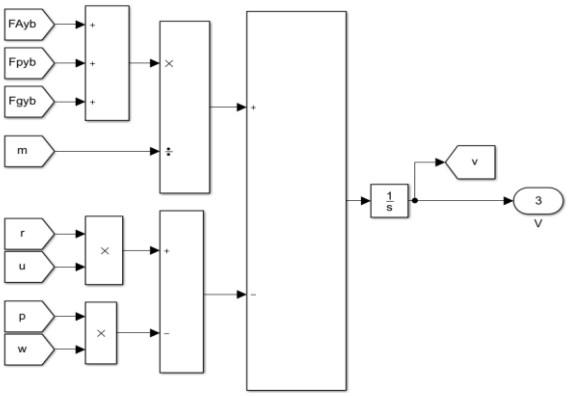

Figure 4.2 Simulation Block of v-Velocity

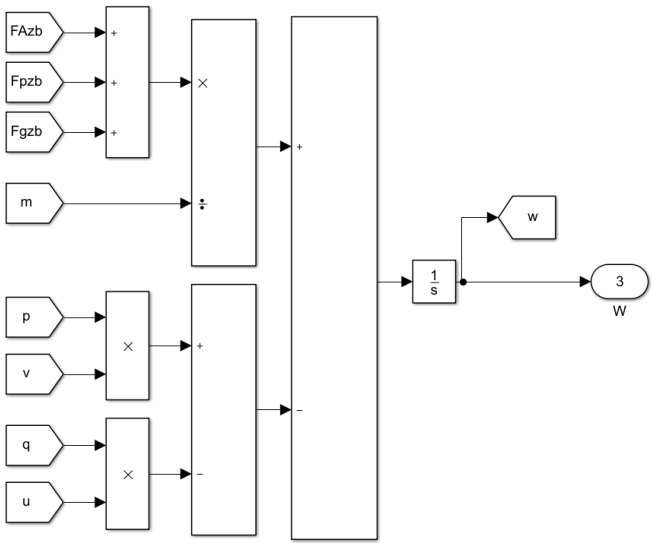

Figure 4.3 Simulation Block of w-Velocity

Also, the rotational parameters of the motion is described using blocks diagrams as shown in Figure 4.4, Figure 4.5 and Figure 4.6

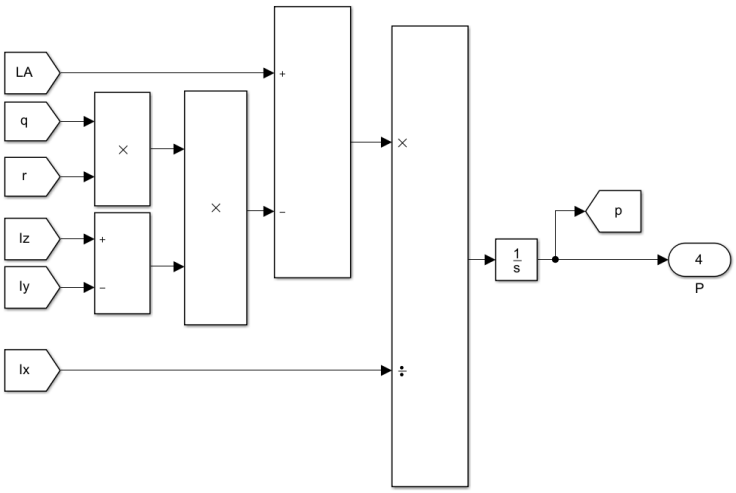

Figure 4.4 Simulation Block of p-Angular Velocity

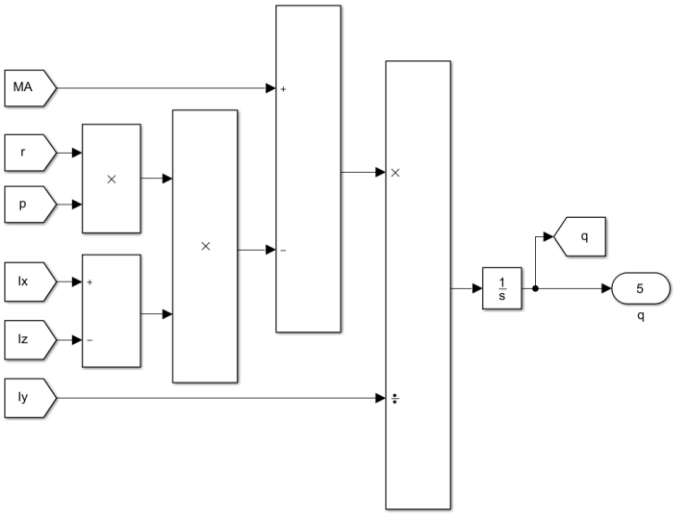

Figure 4.5 Simulation Block of q-Angular Velocity

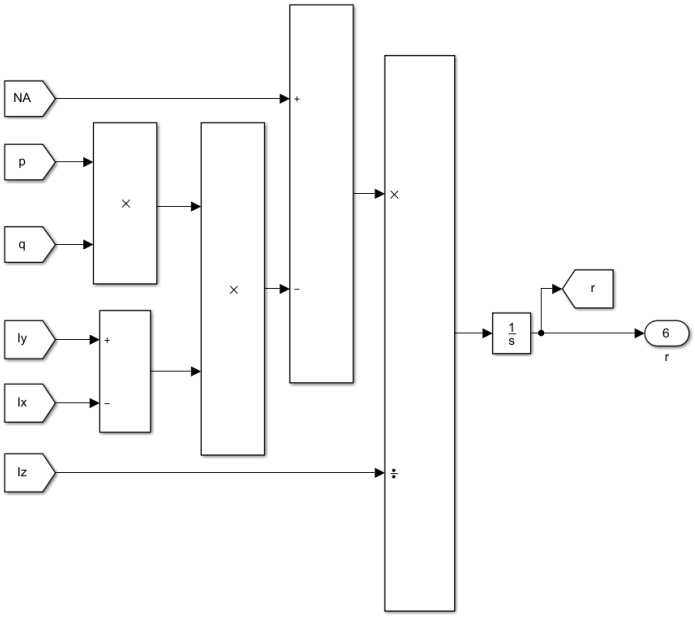

Figure 4.6 Simulation Block of r-Angular Velocity

for Euler angles were described using blocks diagrams as shown in Figure 4.7, Figure 4.8 and Figure 4.9

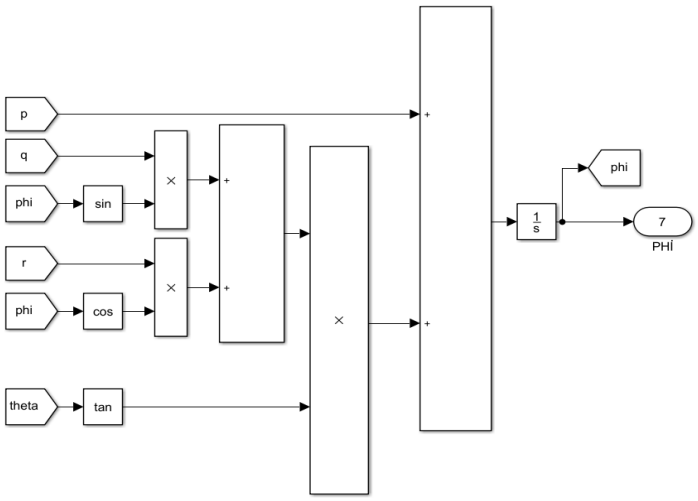

Figure 4.7 Simulation Block of PHI-Euler Angle

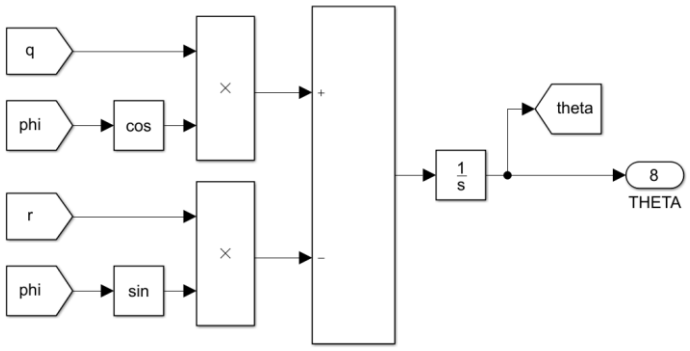

Figure 4.8 Simulation Block of THETA-Euler Angle

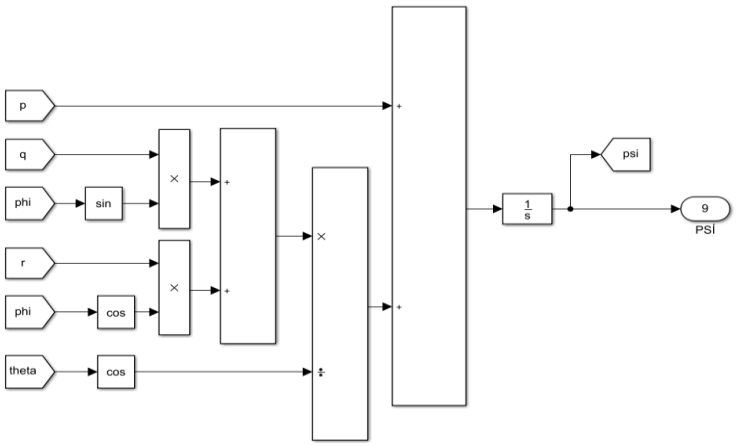

Figure 4.9 Simulation Block of PSI-Euler Angle

The components of aerodynamic forces and moments were also simulated using block diagram as shown in Figure 4.10, Figure 4.11and Figure 4.12

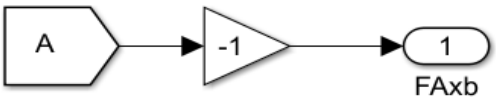

Figure 4.10 Simulation Block of X- Component of Aerodynamic Force

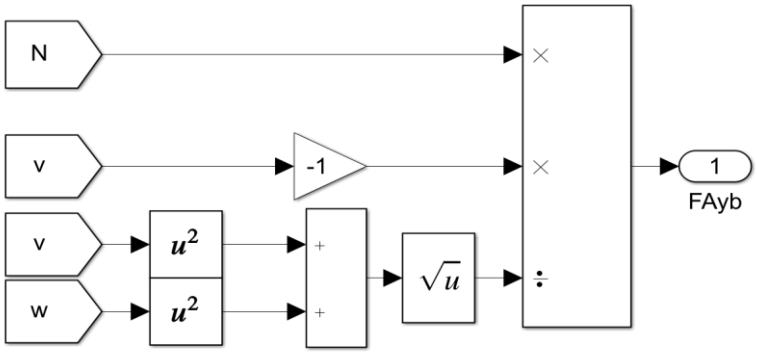

Figure 4.11 Simulation Block of Y- Component of Aerodynamic Force

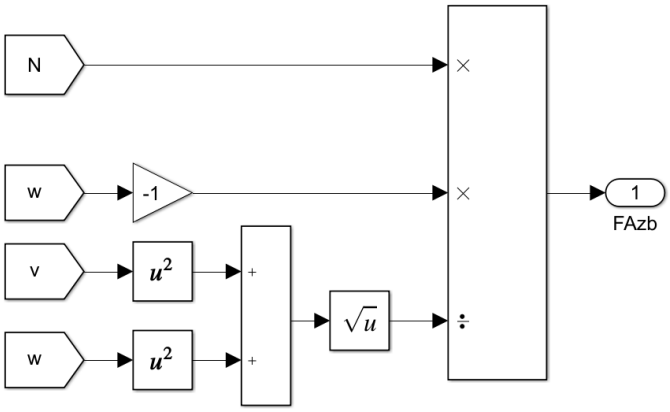

Figure 4.12 Simulation Block of Z- Component of Aerodynamic Force

Simularlly, the aerodynamic axial force a and aerodynamic normal force vector N forces as simulated using the simulink block tool box as shown in Figure 4.13 and Figure 4.14

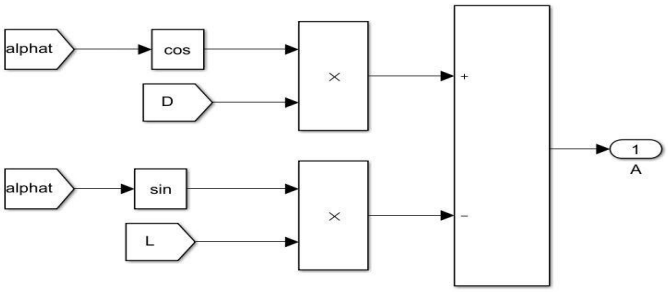

Figure 4.13 Simulation Block of Aerodynamic Axial Force

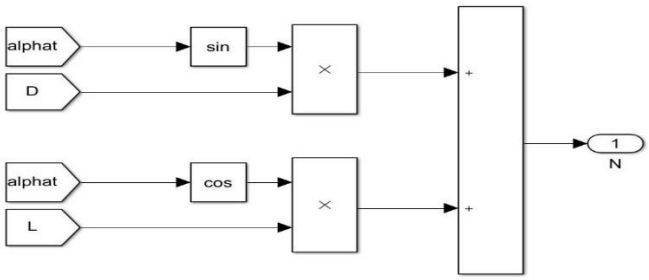

Figure 4.14 Simulation Block of Aerodynamic Normal Force

In the same way, the total angle of attack $\boldsymbol{\alpha t}$ is also simulated using simlukin block box as shown in Figure 4.15

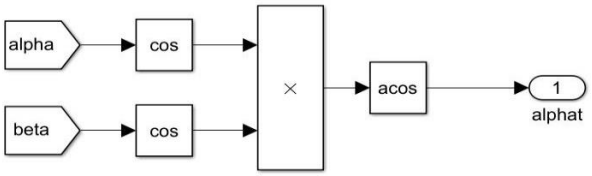

Figure 4.15 Simulation Block of total Angle of Attack

The aerodynamic drag force and aerodynamic lift force were also modelled as shown in Figure 4.16 and Figure 4.17

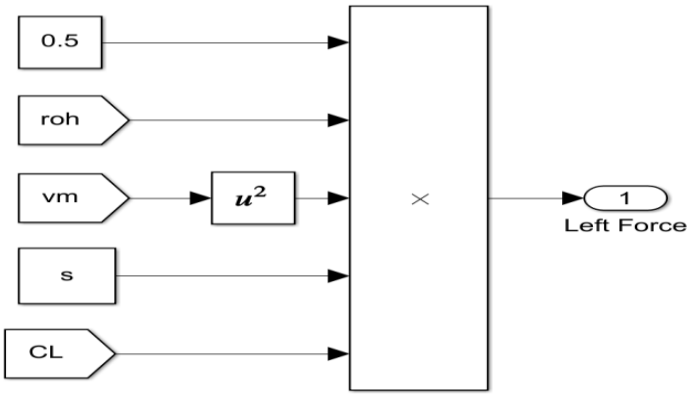

Figure 4.16 Simulation Block of Aerodynamic Lift Force

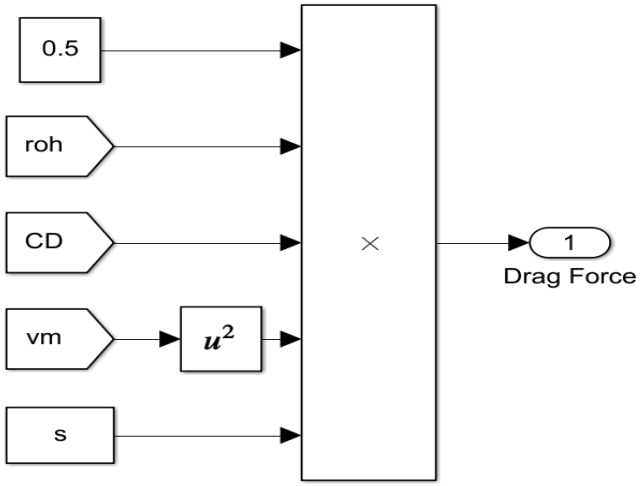

Figure 4.17 Simulation Block of Aerodynamic Drag Force

The aerodynamic drag coefficient C_D and aerodynamic lift coefficient C_L also simulated as shown in Figure 4.18 and Figure 4.19

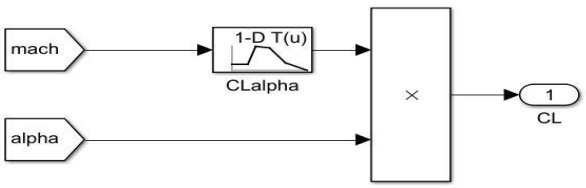

Figure 4.18 Simulation Block of Aerodynamic Lift Coefficient

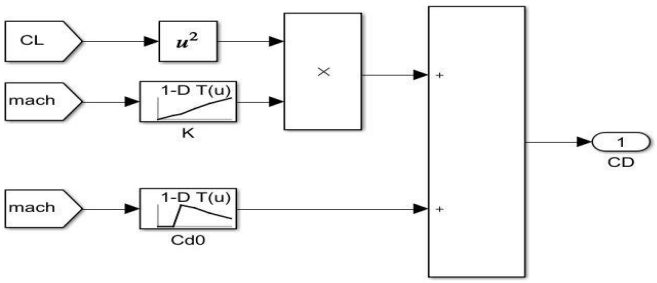

Figure 4.19 Simulation Block of Aerodynamic Drag Coefficient

We should note that (K, C_{D_0} , C_{L_a}) provided to the Simulink as lookup table and it change with Mach number.

In the same way, the aerodynamic moments were simulated as shown in Figure 4.20, Figure 4.21 and Figure 4.22

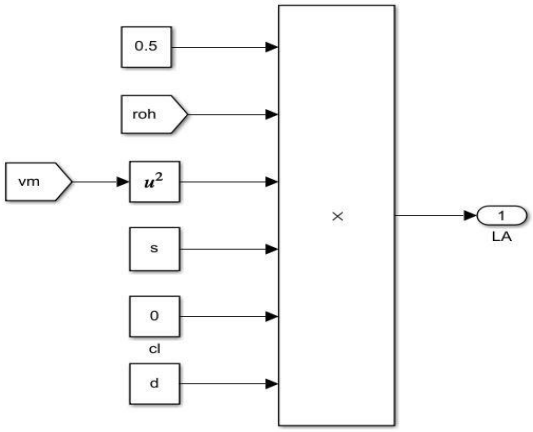

Figure 4.20 Simulation Block of X- Component of Aerodynamic Moment

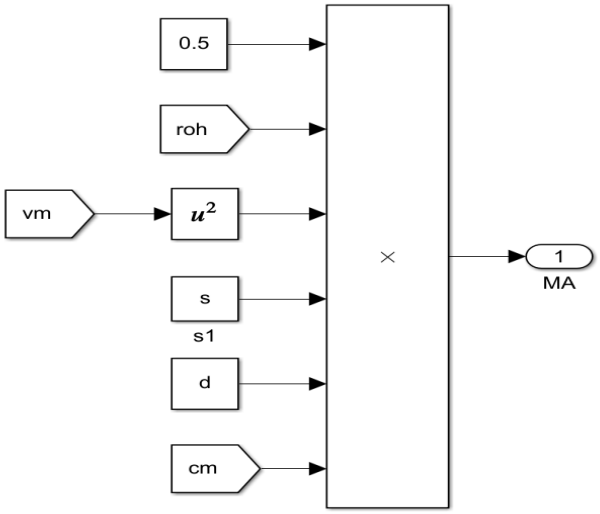

Figure 4.21 Simulation Block of Y- Component of Aerodynamic Moment

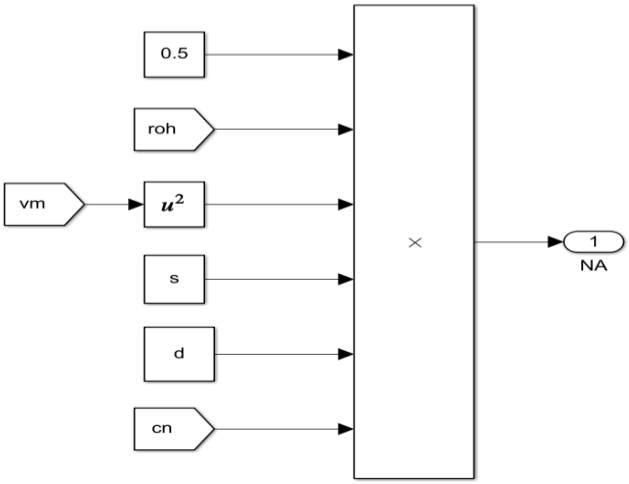

Figure 4.22 Simulation Block of Z- Component of Aerodynamic Moment

Also, the aerodynamic pitch moment coefficient Cm and aerodynamic yaw moment coefficient Cn were simulated as shown in Figure 4.23 and Figure 4.24

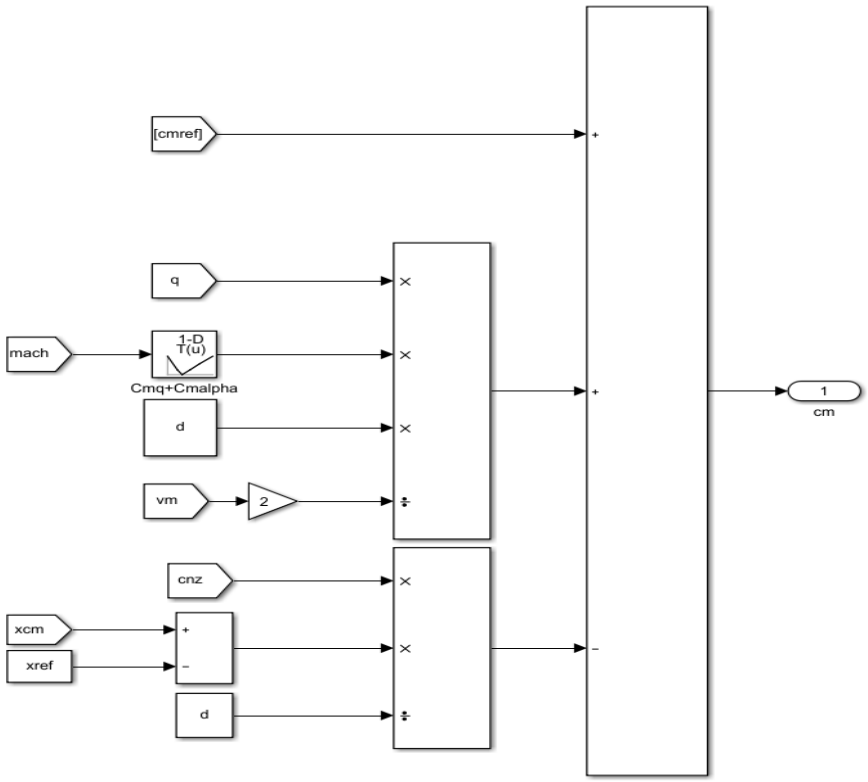

Figure 4.23 Simulation Block of Aerodynamic Pitch Moment Coefficient

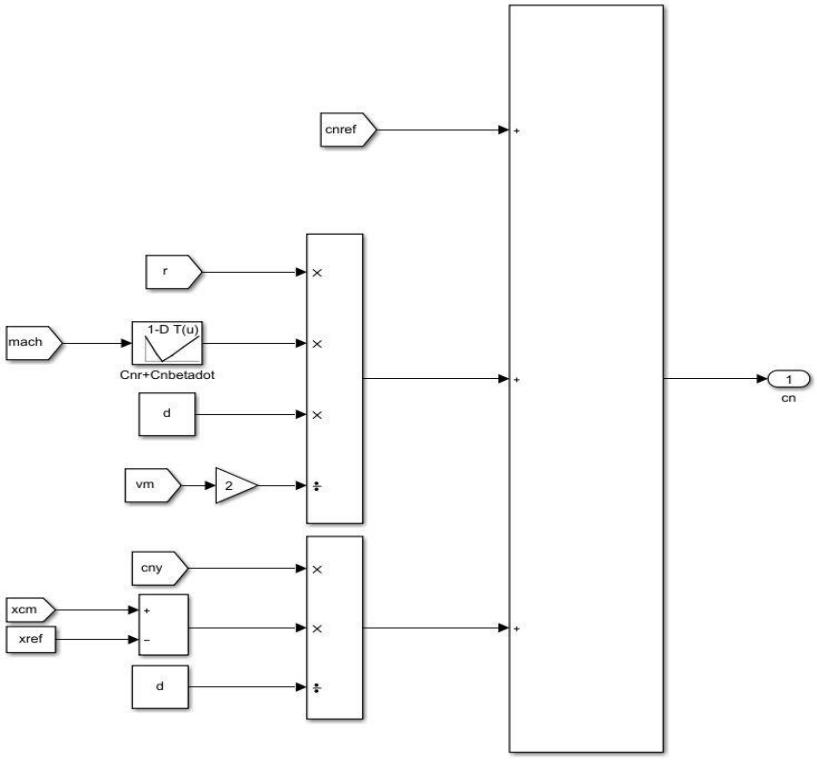

Figure 4.24 Simulation Block of Aerodynamic Yaw Moment Coefficient

The pitch damping $C_{m_q} + C_{m_{\dot{\alpha}}}$ and the yaw damping $C_{n_r} + C_{n\dot{\beta}}$ were entered in simulation using lookup tables.

In the same way, the pitching moment coefficient about reference moment station $C_{m_{ref}}$, yawing moment coefficient about reference moment station $C_{n_{ref}}$ were simulated as shown in Figure 4.25 and Figure 4.26

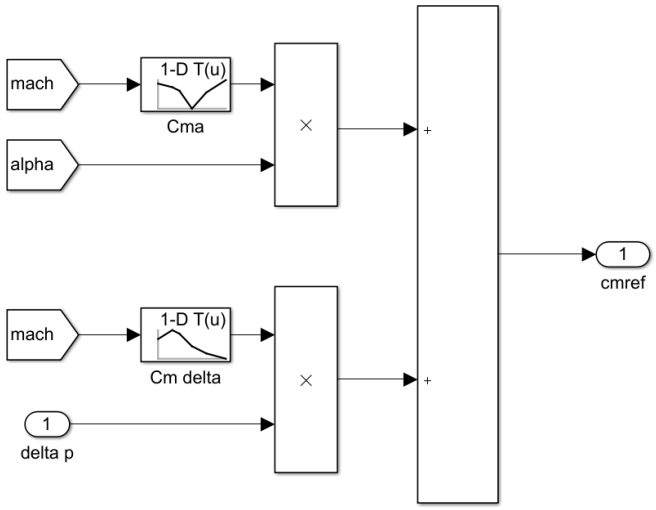

Figure 4.25 Simulation Block of Aerodynamic Pitch Moment Coefficient Around Reference Moment Station

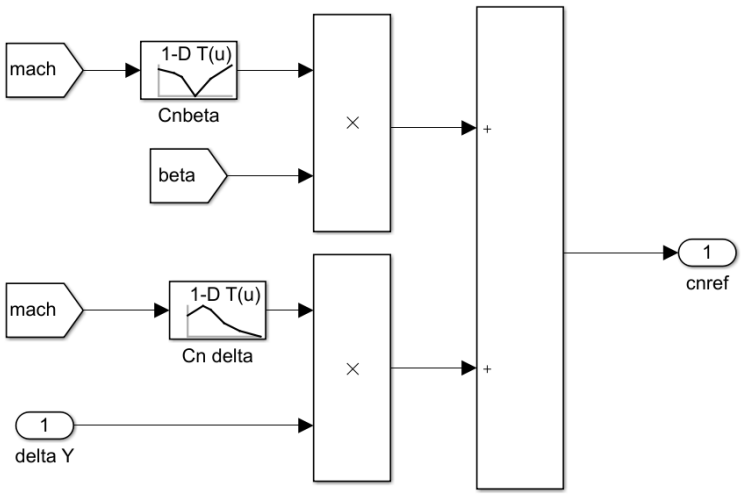

Figure 4.26 Simulation Block of Aerodynamic Yaw Moment Coefficient Around Reference Moment Station

The C_{n_β}, C_{n_δ}, C_{m_δ} and C_{m_a} were provided to the simulation as lookup table.

Finally, the C_{n_y} and C_{n_z} were simulated as shown in Figure 4.27 and Figure 4.28

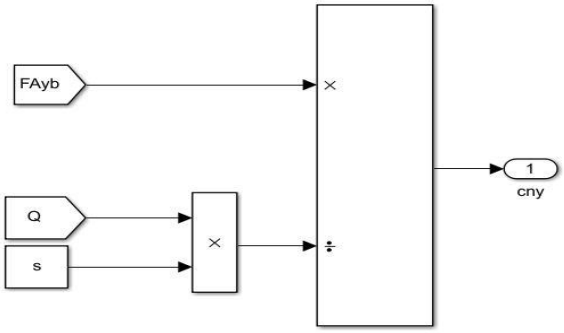

Figure 4.27 Simulation Block of Coefficient Compatible to Normal Force on y_b-axis

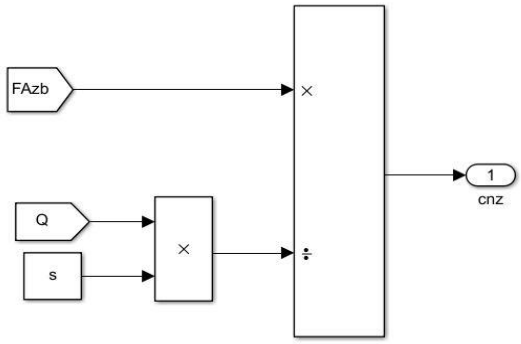

Figure 4.28 Simulation Block of Coefficient Compatible to Normal Force on z_b-axis

The dynamic pressure Q was simulated as shown in Figure 4.29

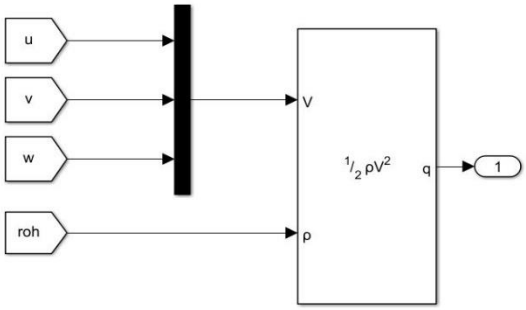

Figure 4.29 Simulation Block of Dynamic Pressure

4.2 the gravity forces

The gravity force should be on the body coordinate, so we used DCM matrix to convert from earth coordinate to body coordinate as shown in Figure 4.30

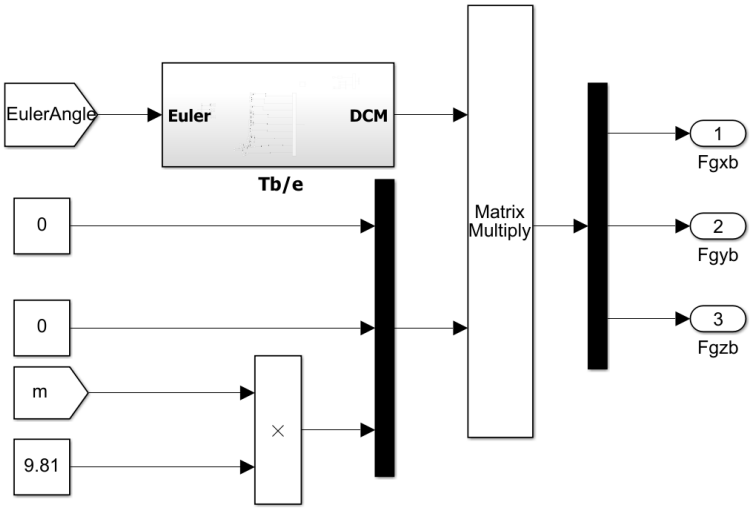

Figure 4.30 Simulation Block of Gravity Forces on Body Coordinate

4.3 Thrust force

The thrust force is parallel to the x- label, and there is no deflection on this simulation as shown in Figure 4.31

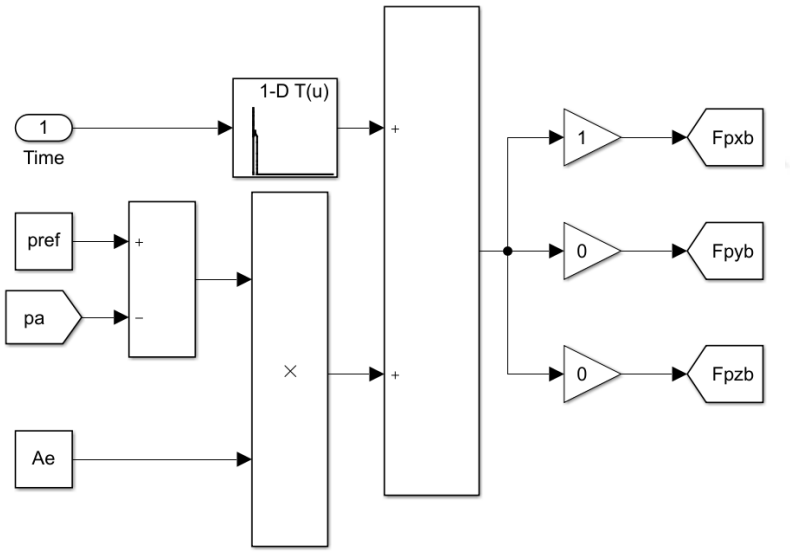

Figure 4.31 Simulation Block of thrust forces on Body Coordinate

4.4 Environmental model and Mach number

The environmental model depend on the height which should be on the earth coordinate as shown in Figure 4.32 and Figure 4.33

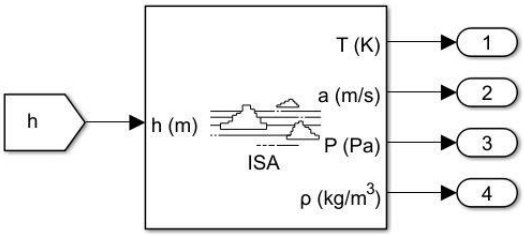

Figure 4.32 Simulation Block of Environmental Model

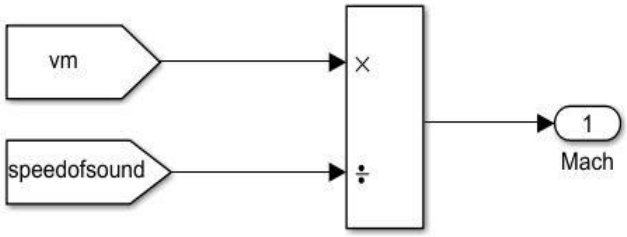

Figure 4.33 Simulation Block of Mach Number

4.5 Time varying parameters simulation

The mass simulation block was simulated as shown in Figure 4.34

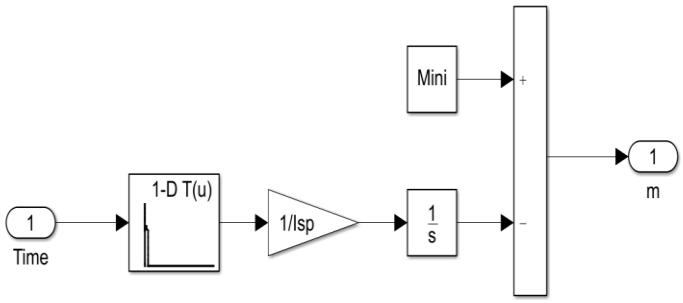

Figure 4.34 Simulation Block of Instantaneous Mass of Missile

also, the center of gravity simulation block was simulated as shown in Figure 4.35

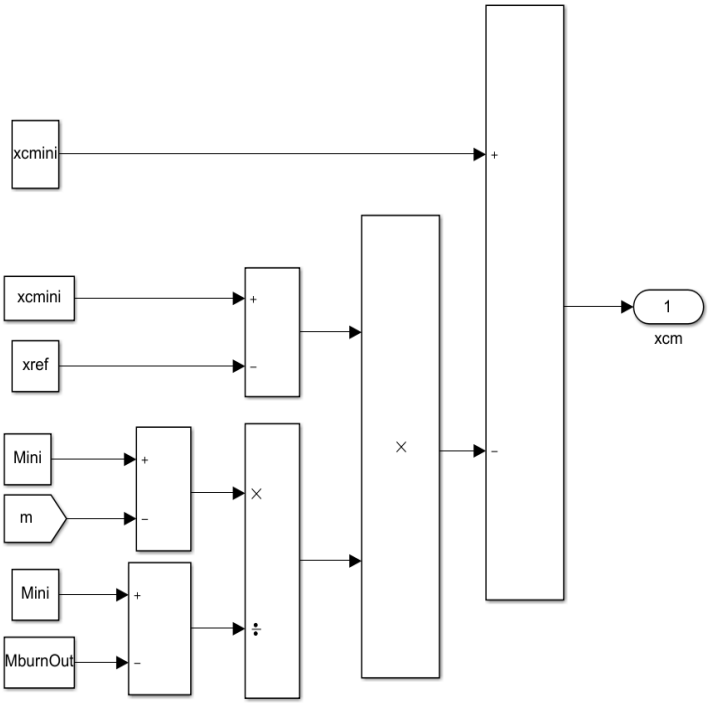

Figure 4.35 Simulation Block of Instantaneous length from Missile Head to Center of Mass

In addition, the moment of inertia simulation blocks were simulated as shown in Figure 4.36, Figure 4.37 and Figure 4.38

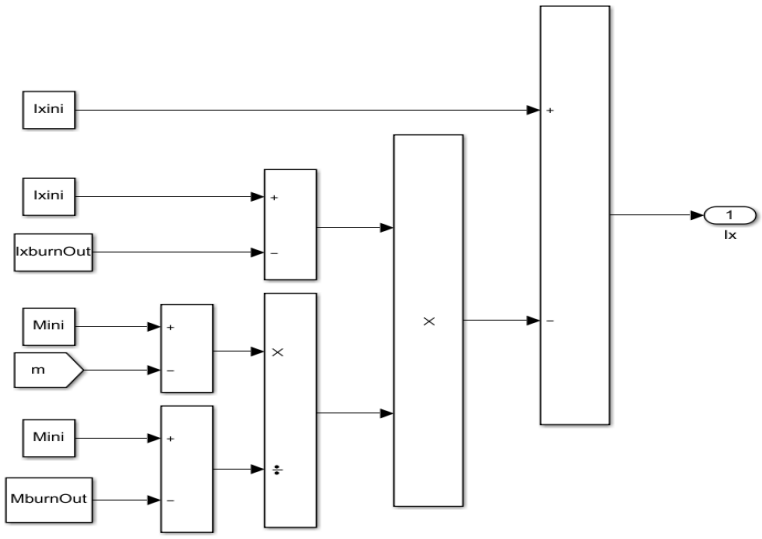

Figure 4.36 Simulation Block of I_x Moments of Inertia

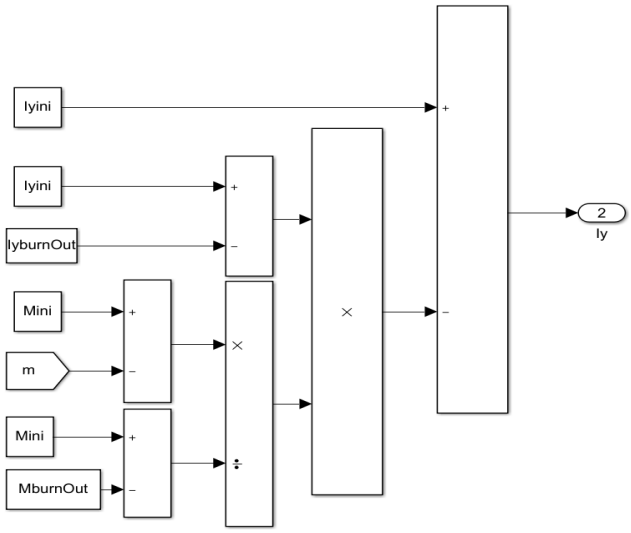

Figure 4.37 Simulation Block of I_y Moments of Inertia

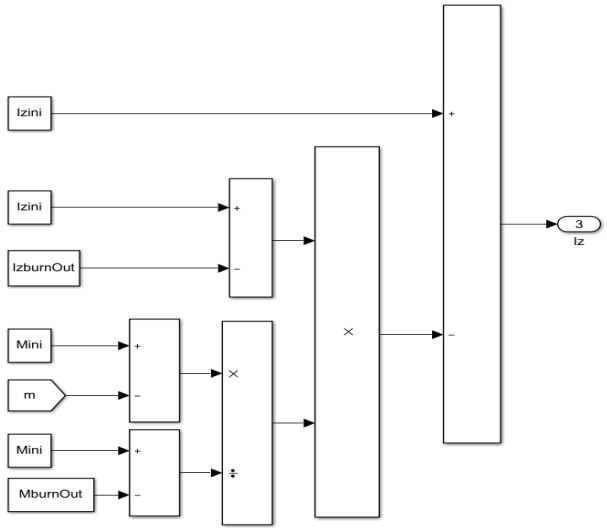

Figure 4.38 Simulation Block of I_z Moments of Inertia

Finally, the Angle of attack, sideslip angle and velocity magnitude were simulated as shown in Figure 4.39

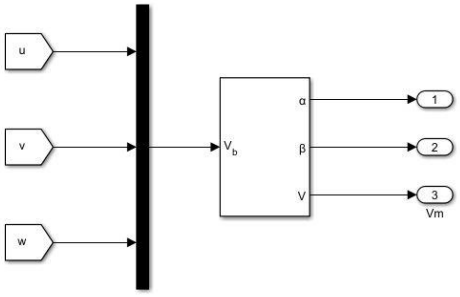

Figure 4.39 Simulation Block of Angle of Attack, Sideslip Angle, Velocity Magnitude

CHAPTER V

CASE STUDY

5.1 Simulation case-study: (Surface to air missile)

For illustrate, it was considered that a specific missile configuration would need to be examined. Canard control surfaces were used to control the missile, the canards and stabilizing tail fins were organized in a cruciform pattern..

The required descriptions for the simulation of the case study were found in textbook of Belkacem & Bachir (2019) which are listed below:

$m_0 = 85.0$ missile mass at launch, kg.

$m_{b0} = 57.0$ missile mass at burnout, kg

x_{cm0} =1.55 the length from head to center of mass at launch, m

x_{cmb0} =1.35 the length from head to center of mass at burnout, m

d = 0.127 aerodynamic reference length (Missile's diameter), m

l =1.6 fuselage length (length from missile tile to center of mass), m

I_0 =moment of inertia around x,y and z axes at launch, kg. m^2

I_{b0} = moment of inertia around x,y and z axes at burnout, kg. m^2

$$[I_{b0}] = \begin{bmatrix} 0.45 & 0 & 0 \\ 0 & 47 & 0 \\ 0 & 0 & 47 \end{bmatrix}$$

$$[I_0] = \begin{bmatrix} 0.7 & 0 & 0 \\ 0 & 61 & 0 \\ 0 & 0 & 61 \end{bmatrix}$$

Table 5.1 Thrust with Time Changing

Time(t)	0	0.01	0.04	0.05	0.08	0.10	0.20	0.30	0.60	1.00	1.50
Trust(ref)	0	450	17800	23100	21300	20000	18200	17000	15000	13800	13300

Time(t)	2.50	3.50	3.80	4.00	4.10	4.30	4.50	4.70	4.90	5.20	5.60	100
Trust(ref)	13800	14700	14300	12900	11000	7000	4500	2900	1500	650	0	0

$t_{b0} = 5.6$ time of burnout, s

$p_{ref} = 101314$ reference ambient pressure, pa

$A_e = 0.011$ exit area of rocket nozzle, m^2

I_{sp}=2224 specific impulse, N.S/kg

V_s =343 speed of sound in elastic medium, m/s

R=287.26 gas constant, N.m/(kg.k)

R_e=6378 earth radius at equator, km

S=0.0127 missile aerodynamic ref area, m^2

D=0.127 aerodynamic reference length, m

$x_{ref} = 1.35$ length from missile head to point of reference for the moment, m

A=lapse rate 6.5×10^{-3} k/m

p_0 =1.2230 air density at sea level kg / m^3

$T_1 = 288.1667 \rightarrow 290k$ Temperature at sea level

Table 5.2 Aerodynamics Parameters Coefficients

COEFFICIENT	MACH NUMBER $M_{n,}$ dimensionless					
	0.0	0.8	1.14	1.75	2.5	3.5
C_{D0}	0.8	0.8	1.2	1.15	1.05	0.94
C_{La}	38.0	39.0	56.0	55.0	40.0	33.0
C_{ma}	-160.0	-170.0	-185.0	-235.0	-190.0	-150.0
$C_{m\delta}$	180.0	250.0	230.0	130.0	80.0	45.0
$C_{m_q} + C_{m_{\dot{a}}}$ $C_{n_r} + C_{n\dot{\beta}}$	-6.000	-13.000	-16.000	-13.500	-10.000	-6.000
k	0.0255	0.0305	0.0361	0.0441	0.0540	0.0665

Normally, the initial conditions (IC), are set for every case study. Therefore, the program made flexible so that it can be entered separately.

In this code, initial conditions are set after leaving the launcher. In other word, the simulation process is started just after leaving the launcher. Thus, for this case study, the following IC were set as follow:

$p_M(i)=0,\ p_M(j)=0,\ p_M(k)=0$

$t_{max}=10$, maximum time of flight, s

$\Delta t=1\times10^{-3}$ integration time step, s

$g_0=9.80665$ acceleration due to gravity m/s^2

$\pi=3.141592654$, dimensionless

$DTR=\pi/180$ factor converting radiance to degrees, dimensionless

$RTD=180/\pi$ factor converting degrees to radiance, dimensionless

$[p,q,r]=0, rad/s(\deg/s)\ \ \alpha=\beta=\alpha_t=0, rad(\deg)$

$m(t=0)=m_0, I(t=0)=I_0, \chi_{cm}(t=0)=\chi_{cm0}$

5.2 Simulation Options

The simulation runs on fixed time mode with 0.0001-time step and ode3 solver, also the variable inserted to the simulation workspace as shown in Table 5.3.

Table 5.3 Input Parameters of Simulation Example

Name	Value	DataType	Dimensions	Complexity	Min	Max	Unit	Argument	StorageClass
Ae	0.011	auto	[1 1]	real	[ ]	[ ]		☐	Auto
Isp	2224	auto	[1 1]	real	[ ]	[ ]		☐	Auto
IxburnOut	0.45	auto	[1 1]	real	[ ]	[ ]		☐	Auto
Ixini	0.7	auto	[1 1]	real	[ ]	[ ]		☐	Auto
IyburnOut	47	auto	[1 1]	real	[ ]	[ ]		☐	Auto
Iyini	61	auto	[1 1]	real	[ ]	[ ]		☐	Auto
IzburnOut	47	auto	[1 1]	real	[ ]	[ ]		☐	Auto
Izini	61	auto	[1 1]	real	[ ]	[ ]		☐	Auto
MburnOut	56.58	auto	[1 1]	real	[ ]	[ ]		☐	Auto
Mini	85	auto	[1 1]	real	[ ]	[ ]		☐	Auto
d	0.127	auto	[1 1]	real	[ ]	[ ]		☐	Auto
phiini	0	auto	[1 1]	real	[ ]	[ ]		☐	Auto
pini	0	auto	[1 1]	real	[ ]	[ ]		☐	Auto
pref	101314	auto	[1 1]	real	[ ]	[ ]		☐	Auto
psiini	0	auto	[1 1]	real	[ ]	[ ]		☐	Auto
qini	0	auto	[1 1]	real	[ ]	[ ]		☐	Auto
rini	0	auto	[1 1]	real	[ ]	[ ]		☐	Auto
roh	1.225	auto	[1 1]	real	[ ]	[ ]		☐	Auto
s	0.0127	auto	[1 1]	real	[ ]	[ ]		☐	Auto
thetaini	0	auto	[1 1]	real	[ ]	[ ]		☐	Auto
uini	10	auto	[1 1]	real	[ ]	[ ]		☐	Auto
vini	0.0001	auto	[1 1]	real	[ ]	[ ]		☐	Auto
wini	0.0001	auto	[1 1]	real	[ ]	[ ]		☐	Auto
xcmini	1.55	auto	[1 1]	real	[ ]	[ ]		☐	Auto
xref	1.35	auto	[1 1]	real	[ ]	[ ]		☐	Auto

5.3 Simulation Results:

This code allows to plot the mass variation versus time for 10 second, where the mass change from 85kg to 0, as shown in Figure 5.1

Also, the components of the moment of inertia were also plotted as shown in Figure 5.2

In addition, the results of the calculation were found for length from missile head to the center of mass with time, Mach number, velocity components, absolute velocity, dynamic pressure, angular velocity, Euler angle, angle of attack and sideslip angle as shown in Figure 5.3, Figure 5.4, Figure 5.5, Figure 5.6, Figure 5.7, Figure 5.8, Figure 5.9 and Figure 5.10 respectively .

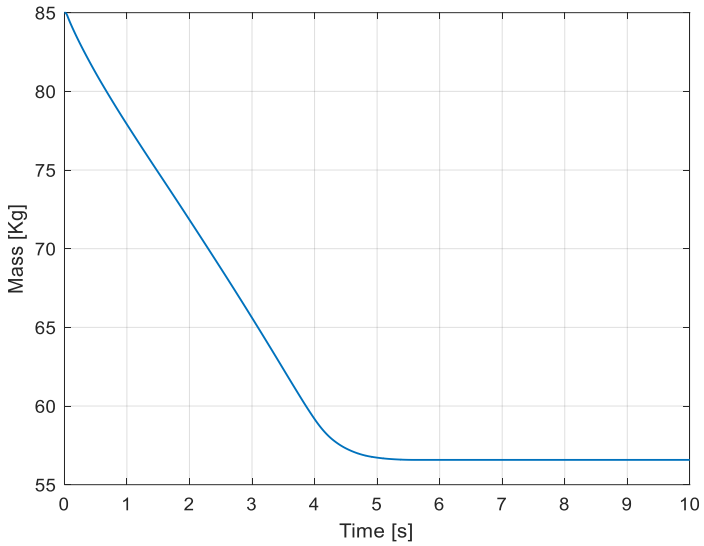

Figure 5.1 Results of Mass Variation with Time

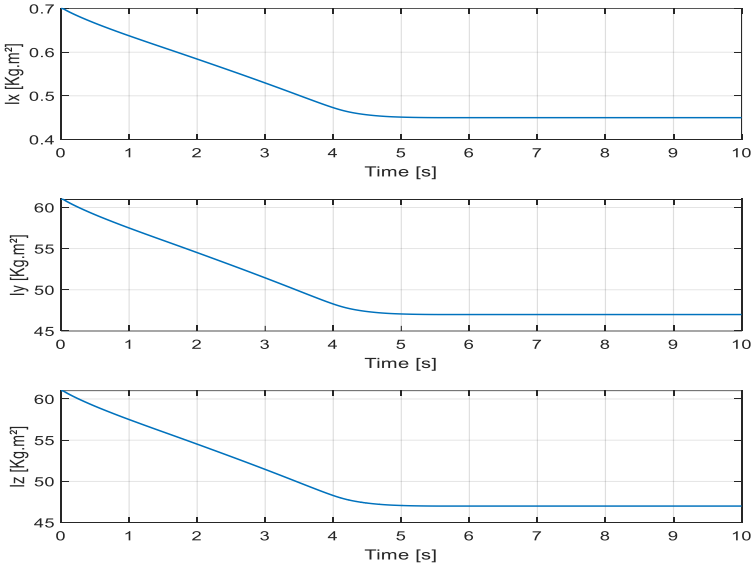

Figure 5.2 Results of Moment of Inertia with Time

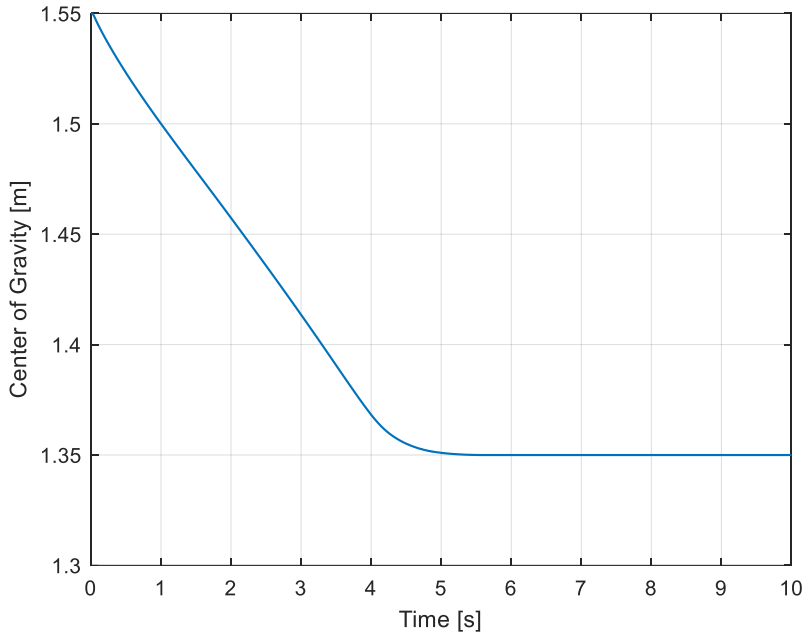

Figure 5.3 Result of Length from Missile Head to Center of Mass with Time

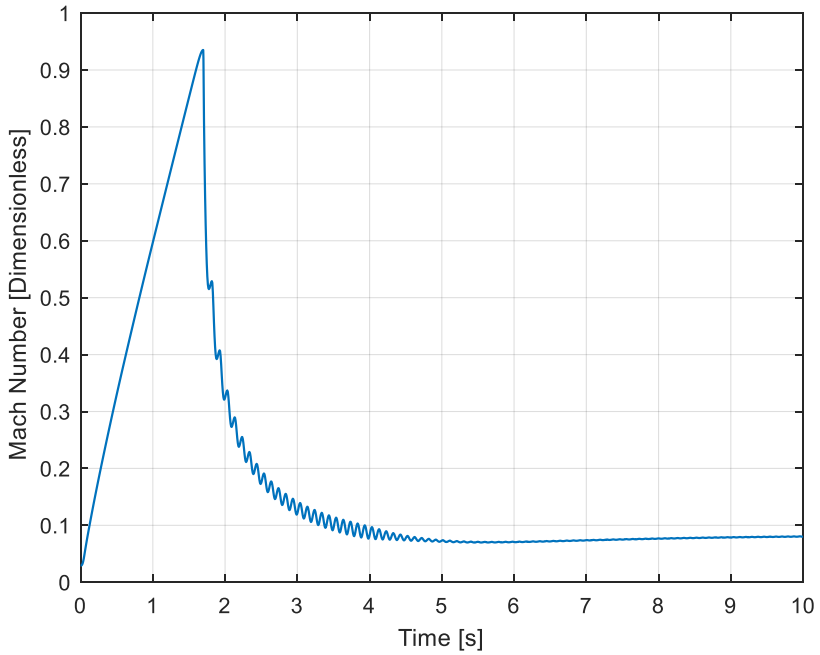

Figure 5.4 Result of Mach Number Variation with Time

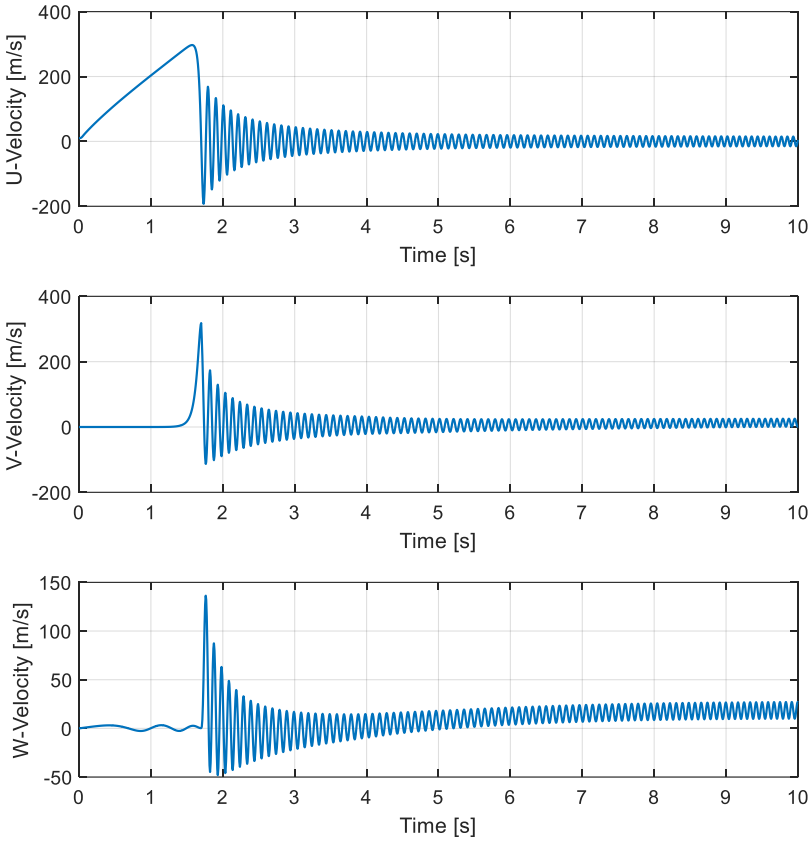

Figure 5.5 Results of Velocity Components Variation with Time

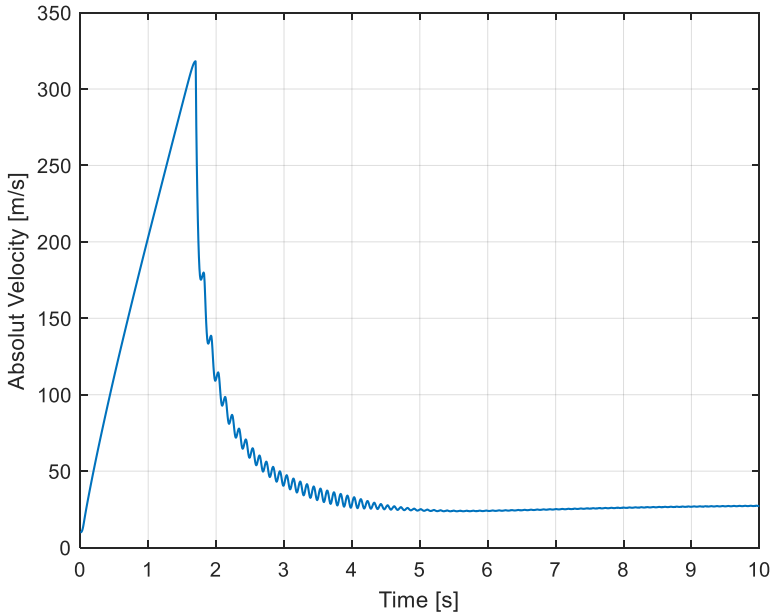

Figure 5.6 Result of Absolute Velocity Variation with Time

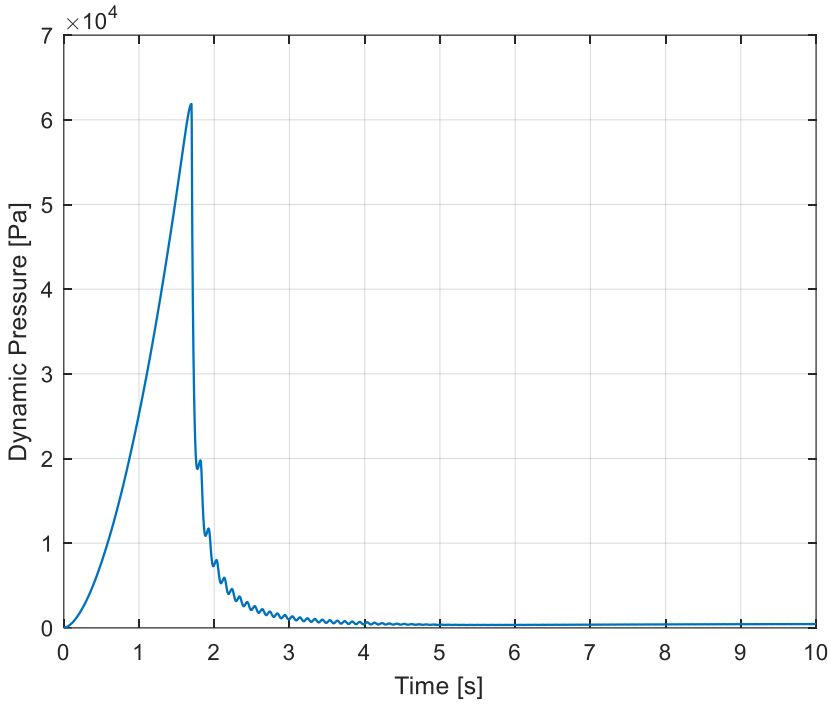

Figure 5.7 Result of Dynamic Pressure Variation with Time

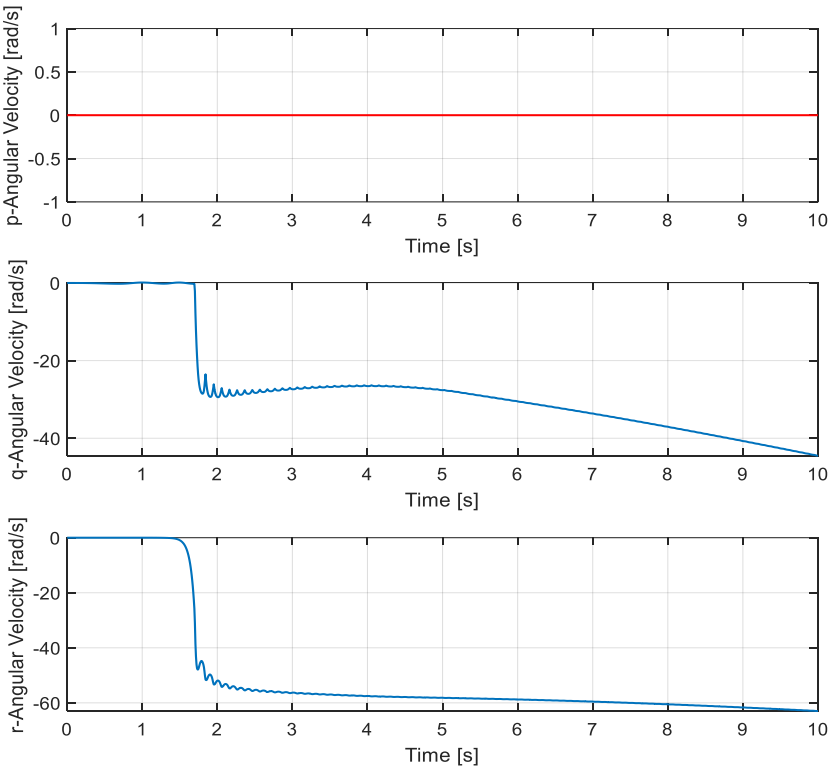

Figure 5.8 Result of Angular Velocity Variation with Time

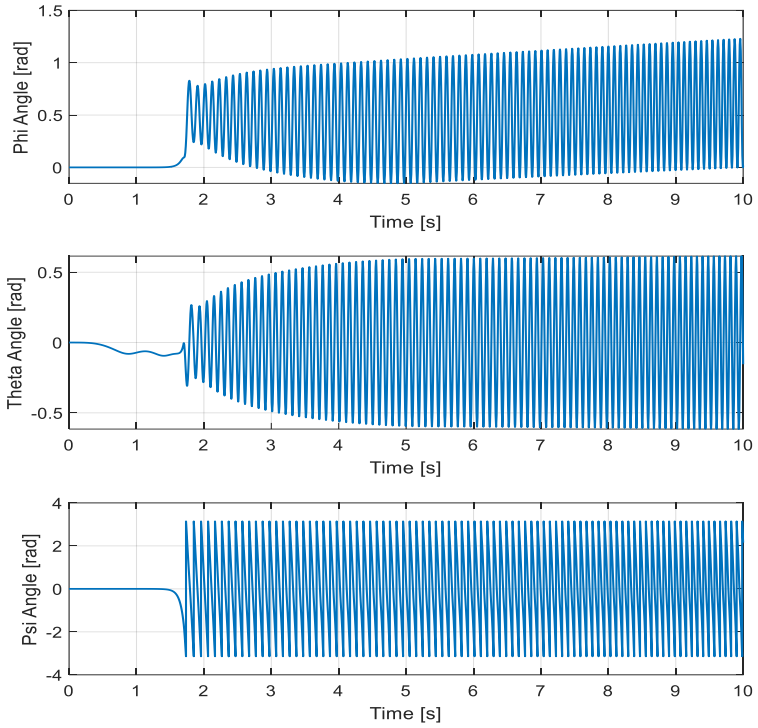

Figure 5.9 Result of Euler Angle Variation with Time

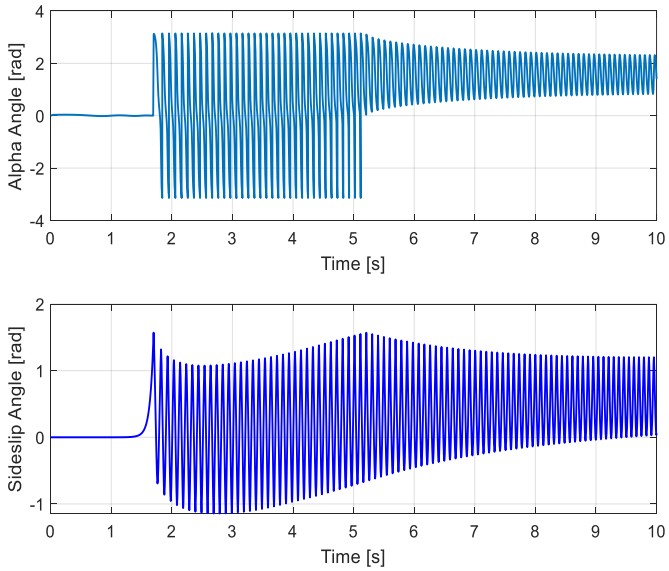

Figure 5.10 Results of Angle of Attack aand Sideslip Angle Variation with Time

The plots shows that the studied missile was not stable, therefore, it was necessary to design a stabilizer using PID stabilizer and tuning it using Ziegler- Nichols method.

CHAPTER VI

STABILIZER DESIGN

6.1 Ziegler-Nichols Method

For a large range of common industrial applications, Ziegler-Nichols closed-loop calibration has been largely viewed as a reasonably good heuristic way to determine optimal settings of PID and PI controllers. (Hang et al., 1991). However, because it is difficult and time consuming . This manual tuning method is rarely used in practice. It also demands the control engineer's attention, as the process must be run around the stability area in order to evaluate the ultimate gain and period.

Since 1981, a variety of software programs for automatic optimization and adaptive control have been offered.Currently, a basic auto tuning mechanism has been invented .It is based on automatic evaluation of the ultimate gain and period from which the appropriate PID and PI controller parameters are frequently calculated using the Ziegler-Nichols tuning method.

Because it can be complemented by fine-tuning based on experience, the Ziegler-Nichols modulation formula has been proven to be quite sufficient in manual adjustment. with the automation of the controller-tuning method, the possibility of altering or augmenting the tuning formula by using heuristic information to replace manual fine tuning becomes appealing.

6.2 Ziegler-Nichols Formula

The Ziegler-Nichols tuning method is based on scientific understanding of ultimate gain Ku and ultimate period Tu (Hang et al., 1991), so for PID controller:

Proportional gain $k_c = 0.6\ K_u$

Integral teime $T_i = 0.5\ T_u$

Derivative time $T_d = 0.125\ T_u$

Also we know that:

$$k_i = \frac{k_p}{T_i}$$

$$k_{d=} k_p T_d$$

6.3 Case Study:

For our example and to control pitch angle, θ, and yaw angle, ψ, we note that:

k_u =15, T_u= 0.17

Then:

k_p= k_c =9

T_i=0.085, K_i=105.88

T_d=0.02125, K_d=0.19125

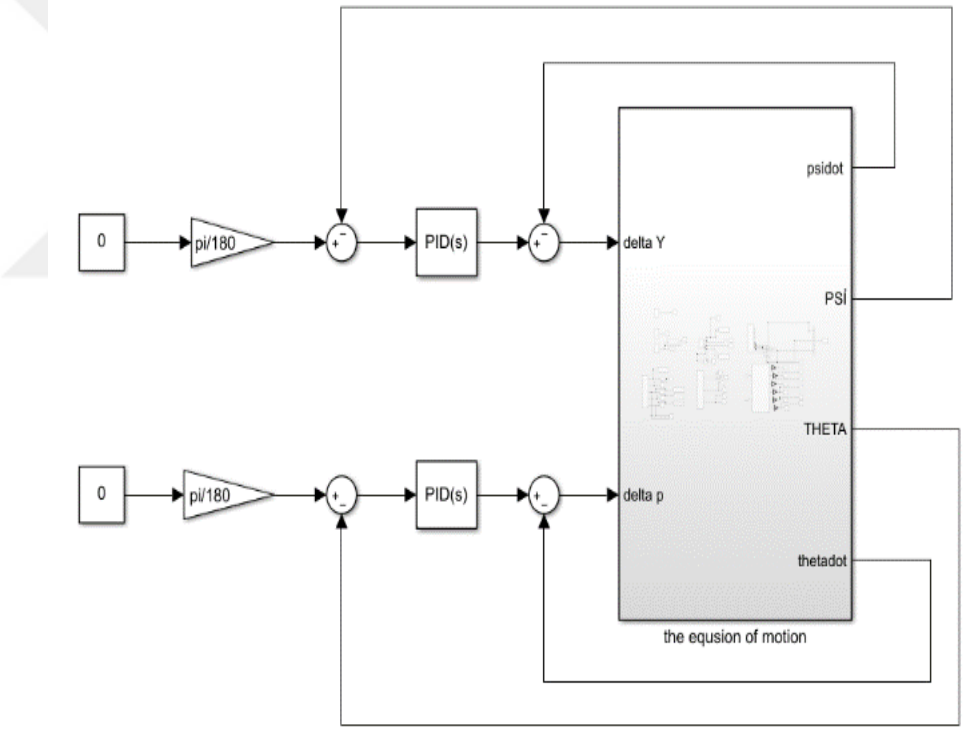

Figure 6.1 Simulation Block of Missile Model with the Stabilizer

after designing the PID controller depending on Ziegler-Nichols method as shown in Figure 6.1, the results of missile performance were calculated as shown in Figure 6.2, Figure 6.3,

Figure 6.4 and

Figure 6.5.

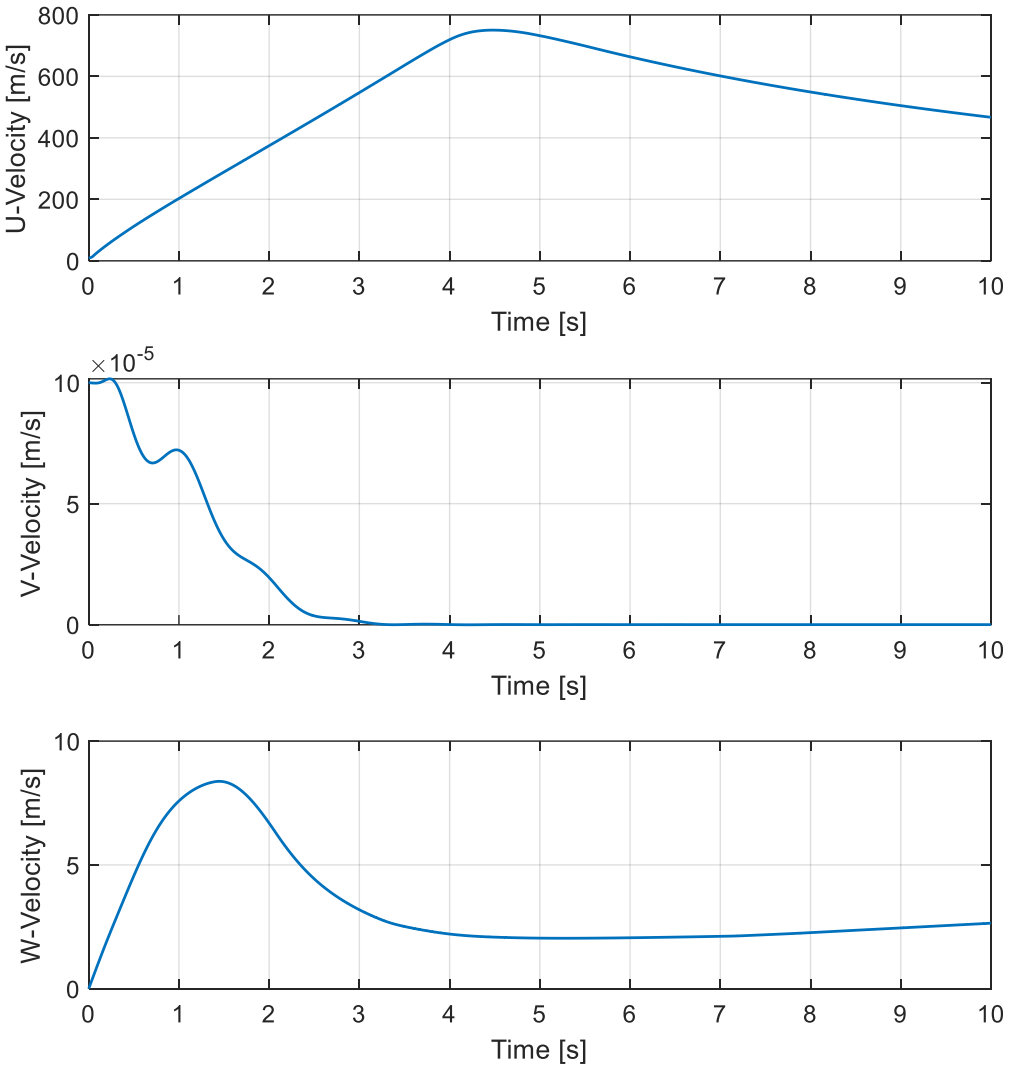

Figure 6.2 Results of Velocity Components Variation with Time, after Designing the Stabilizer

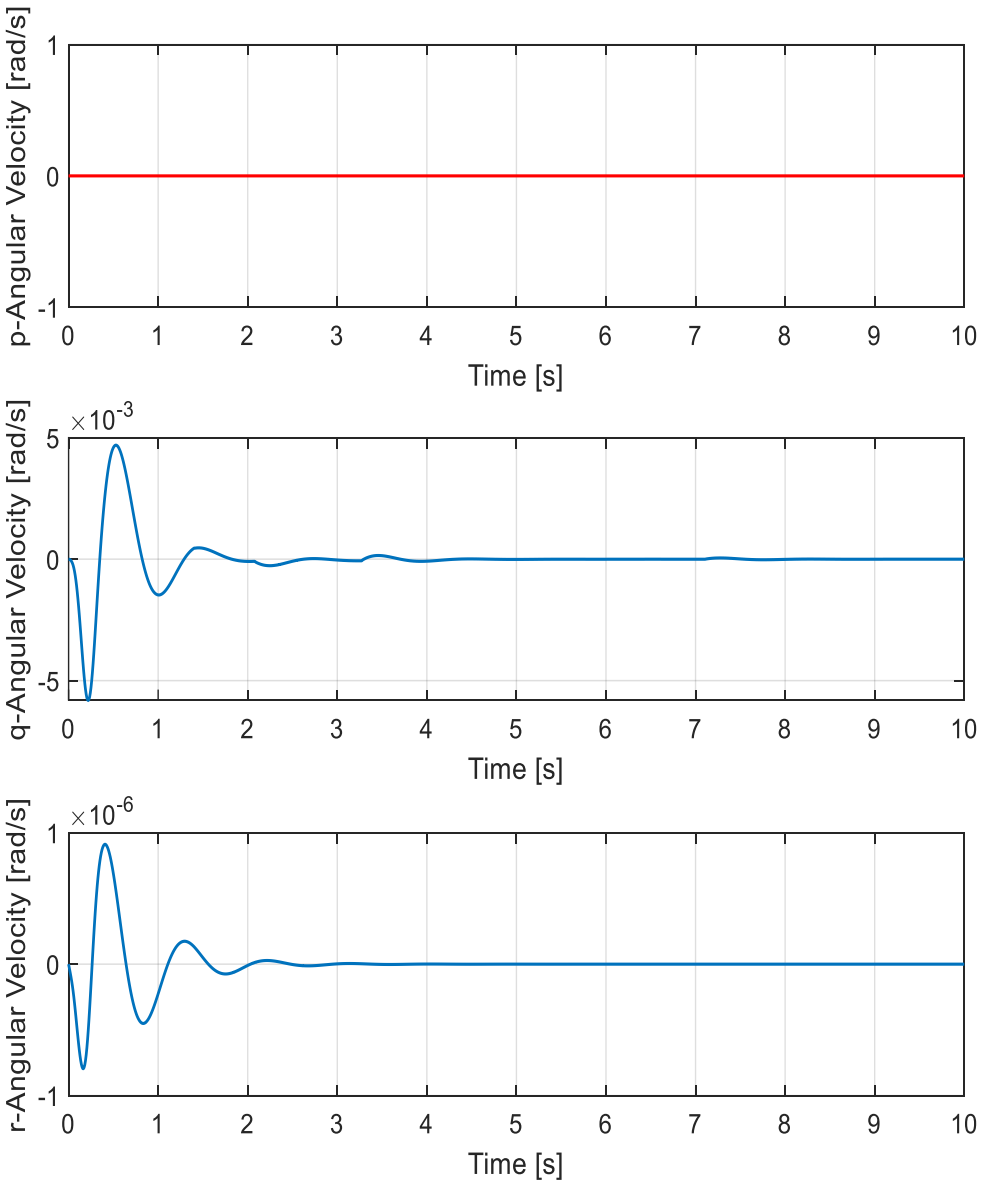

Figure 6.3 Results of Angular Velocity Components Variation with Time, after Designing the Stabilizer

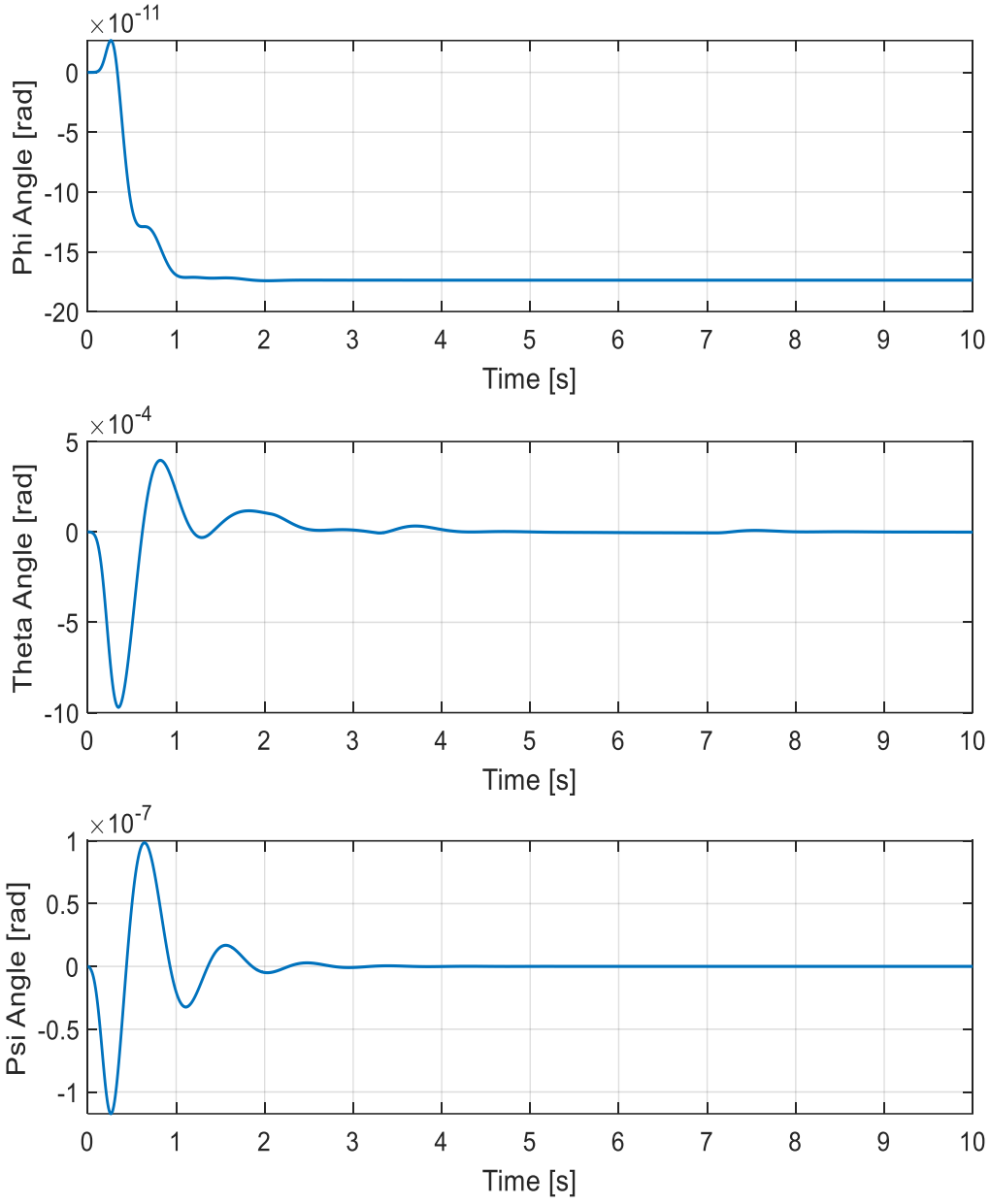

Figure 6.4 Results of Euler Angle Variation with Time, after Designing the Stabilizer

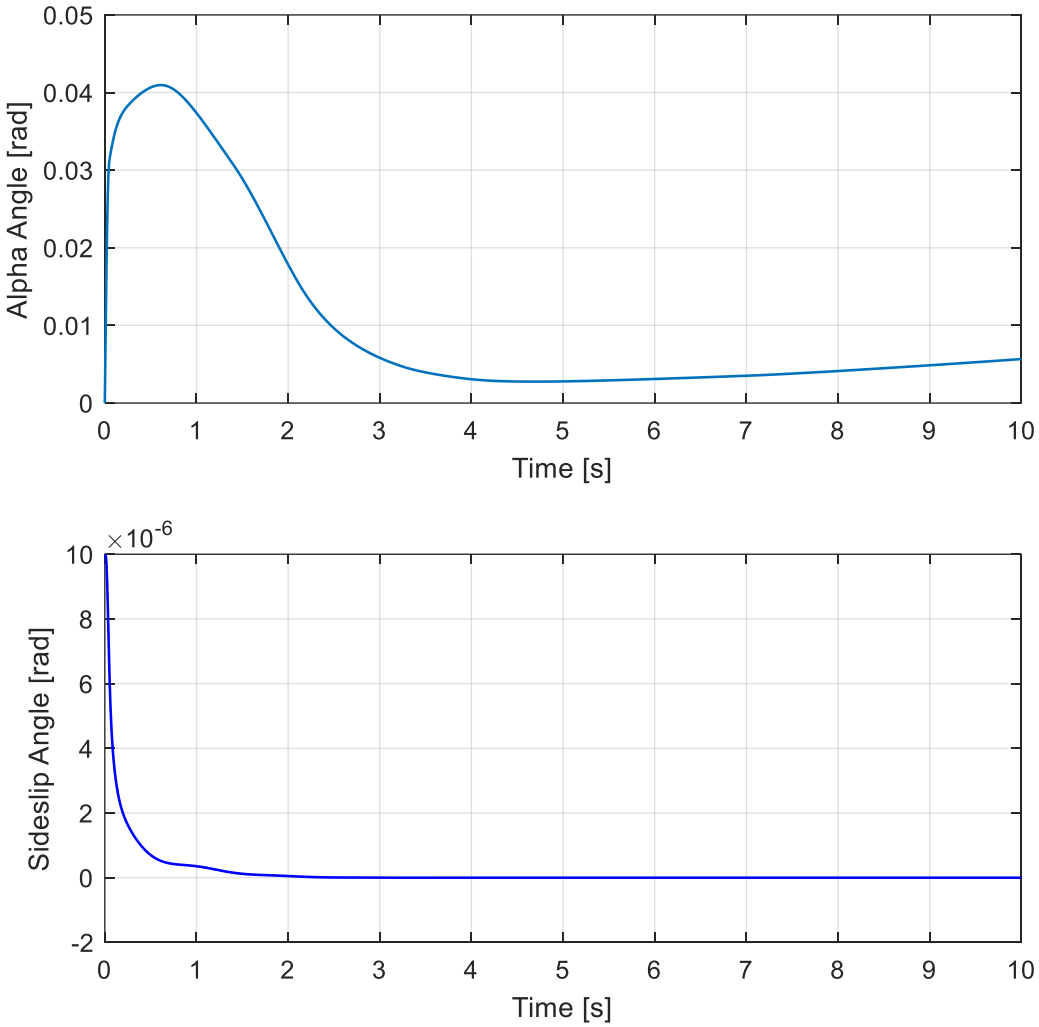

Figure 6.5 Results of Angle of Attack aand Sideslip Angle Variation with Time, after Designing the Stabilizer

It is noted from the results after designing the stabilizer that the oscillation signal has been removed and the output become stable .

CHAPTER VII

MODEL VERIFICATION

7.1 Model Verification

Operators of a missile flight simulator should trust that the simulation findings are accurate and the output is realistic of actual missile behavior. This assurance is acquired via the verification and validation procedures. (Murri et al., 2015).

Validation evaluates the amount to which the simulation is a realistic depiction of the real world, while Verification guarantees that the computer algorithm runs correctly respect to the conceptual framework of the rocket system. It must be proved, in particular, that the missile performance variables that are most important to the simulation goals are simulated with an appropriate level of authenticity. Acceptability limits can be rather broad for less crucial parameters and quite narrow for more critical ones. Verification is essentially an error checking process that ensures logic sequences are working as intended and the program accurately represents the model equations

Inspection of the software program, comparison with other simulations, evaluating specific simulation modules versus recognized or acceptable standards, and ensuring that all logic steps are evaluated for accuracy are all examples of verification methods. Verification is essentially an error checking process of making sure logic patterns are working as intended, the program closely matches the mathematical models, hardware component devices are handled correctly, and simulated system and subsystem characteristics are proportionate with the conceptual model depection and specifications.

on the other hand, Scientific consensus, matching with previous data, comparison with testing data, peer review, and independent review are examples of validation methods. (Cover, 1995).

So in this thesis, to verificate the simulation it was relied on the published results to be certain that the simulated program establishing an adequate agreement between the computational results of the model and data collected from real system tests or other

credible sources, confirming that the missile system and surrounding simulation is appropriate to its intended purpose.

The Figure 7.1 which has been taken from my simulation and Figure 7.2 which has been taken from (Cover, 1995)Showed good agreement in the absolute velocity, so my simulation works properly, and the program adequately represents the model equations. It is also appropriate for its intended purpose, as evidenced by the acceptable agreement among the numerical simulation..

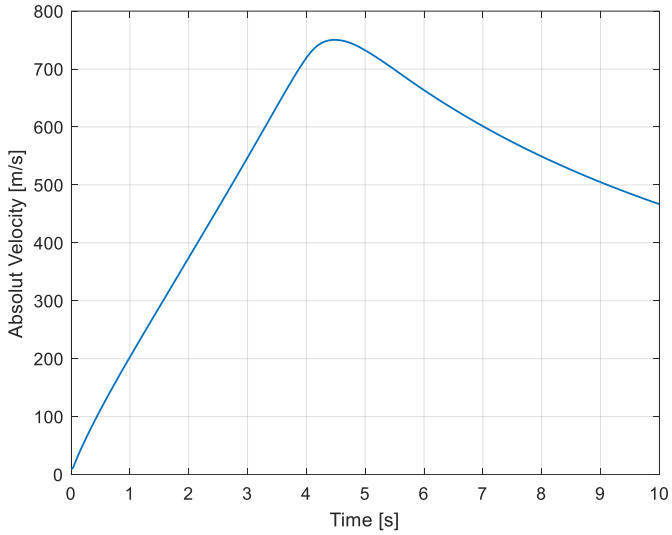

Figure 7.1 Results of Absolut Velocity Variation with Time, after Designing the Stabilizer

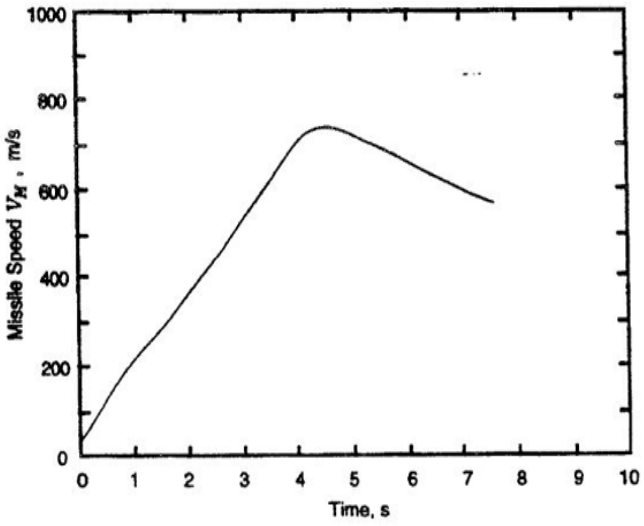

Figure 7.2 Results of Absolut Velocity Variation with Time, from Military Handbook(Cover, 1995)

CHAPTER VIII

MOVED TARGET

8.1 Moved Target

In short, the same equations of motion, which explain missile's flight, also is applicable to a flying target.However, in a missile motion simulator, the equations,which were used to determine target movement, are roughly approximated. The target's flight behavior is generally unimportant for the aim of this study, but it simulated to ensure that the simulated target motion is accurate enough to satisfy the missile flight simulation aims (*Military Handbook. Missile Flight Simulation. Part one. Surface-to-Air Missiles (z-Lib.Org).Pdf*, n.d.). As a result, if the goal of the simulation is to determine the greatest defended area covered by a specific surface-to-air missile, constant-speed target flight paths might suffice. However, if the missile's performance is to be investigated when it engages a certain type of aircraft that conducts precise maneuvers, a more data for the target is required.

8.2 Relative Missile-Target Geometry:

The related distance vector R is a vector that runs from the missile's center of mass to the event's center of gravity. If the length between the seeker of missile and the missile's center of mass is neglected, the seeker tracking and miss distance are calculated using the related distance vector.

This is calculated using the following formula in the coordinate frame of earth:

$$R = P_T - P_M \tag{8.1}$$

$$\psi = \mathrm{Tan}^{-1}\left(\frac{r_x(0)}{r_y(0)}\right) \tag{8.2}$$

$$\theta = \mathrm{Tan}^{-1}\left(\frac{-r_z(0)}{\sqrt{r_y(0)^2 + r_x(0)^2}}\right) \tag{8.3}$$

$$\vec{R} = \begin{pmatrix} r_x \\ r_y \\ r_z \end{pmatrix} = \frac{\vec{R}}{\left\|\vec{R}\right\|} = \frac{P_T - P_M}{\left\|P_T - P_M\right\|} \tag{8.4}$$

8.3 Numerical Results for Missile and Target Motion

For hypothetical scenario the target has following flight parameter:

$P_T(i)$= 4 km, $P_T(j)$= 1 km, $P_T(k)$= -3 km

$V_T(i)$= -250 m/s, $V_T(j)$= 0 m/s, $V_T(k)$= 0 m/s

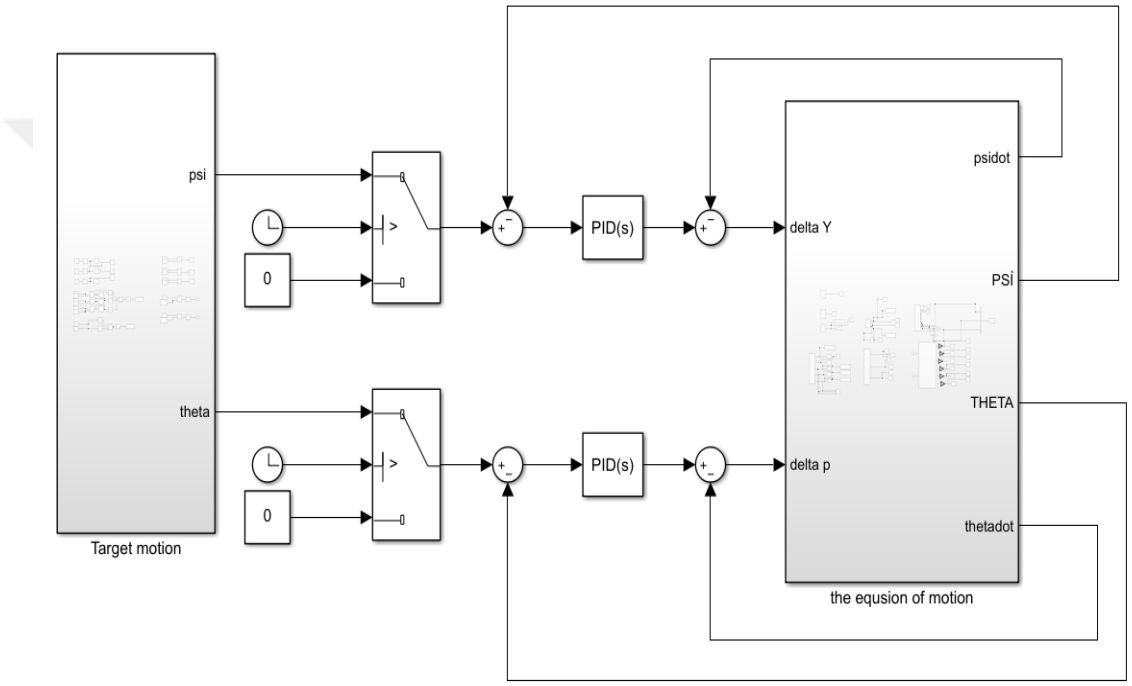

Figure 8.1 target motion with missile model

Switch block added to the simulation to ensure that the missile will receive the control signal after certain time, while the missile get velocity as shown in Figure 8.1

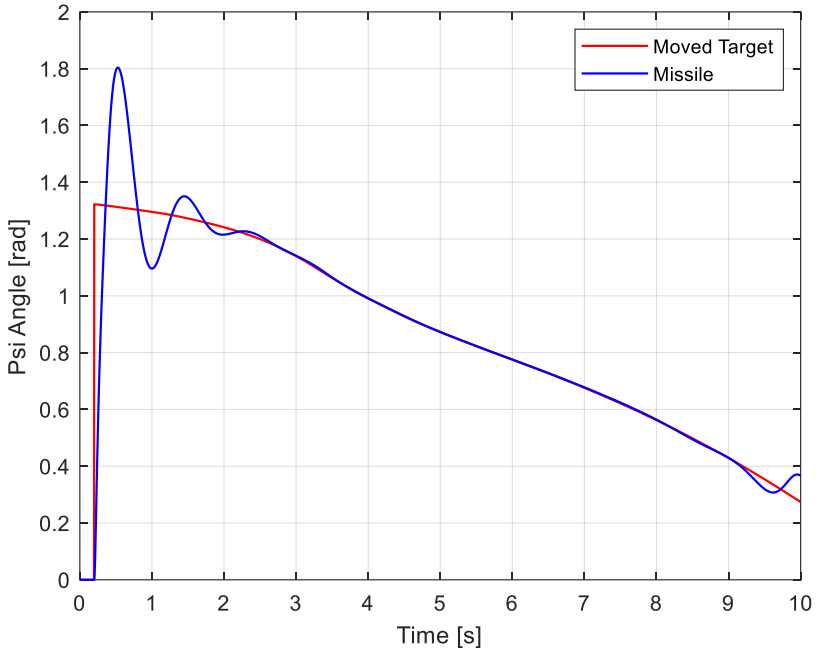

Figure 8.2 Missile and Target Scenario For Psi Angle

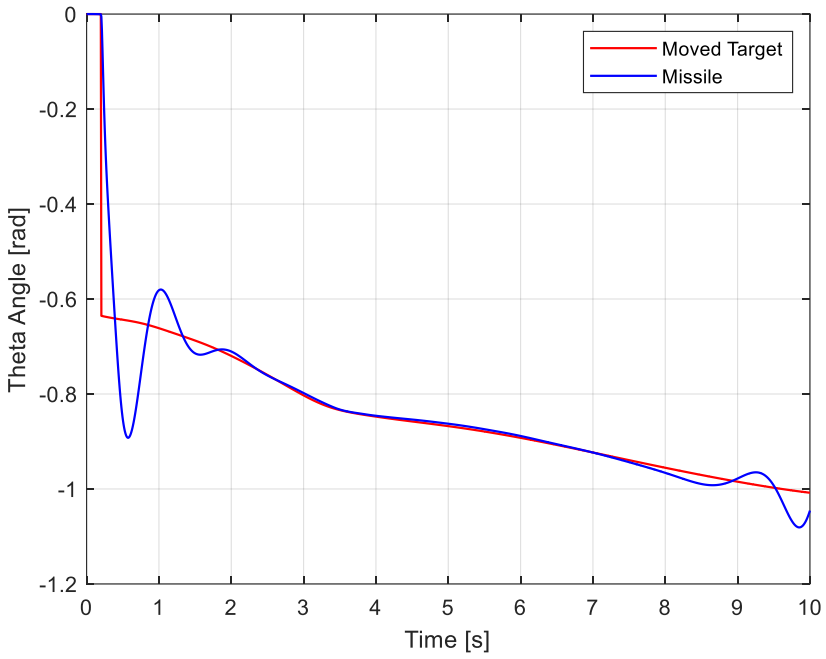

Figure 8.3 Missile and Target Scenario For theta Angle

It is noted that in the end of the simulation there is a difference between the missile angles and target angle as shown in Figure 8.2 and Figure 8.3, however, this happen because the missile velocity drops down.

CHAPTER IX

CONCLUSION AND RECOMMENDATIONS

In this project, flight simulator for a generic missile was developed using SIMULINK. a case study of a canard missile was analyzed using the developed simulator. Full set of data of the case study was found in the literature in terms of Thrust, inertia tensor, aerodynamics stability and control derivatives found. For validation, the time series of the resulted absolute velocities were plotted and compared with the same result that found in the literature. The comparison showed good agreements.

During the development of this work the following conclusions were found Lack of literature containing aerodynamics of missile or data that only applies to narrow angles of attack or data that only applies to certain zones of Mach number, however, to get the aerodynamic parameters, it must be used the FSI method by using ANSYS software because the semi empirical software like missile. DATCOM is restricted for United State of America, but the FSI method needs a super computer to solve this problem, so it was intended to get the aerodynamic parameters directly from the literature when it was found that it is for canard missile because it could not be found full parameters for satellite missile (expandable launch). So, to get the aerodynamic parameters, it needs a separated work.

The simulator allowed to design a PID controller easily and to use Ziegler-Nichols method to perform the tuning process. This approach showed flexibility in modelling and controlling without the need to the linearity process. Then the same code is used to target a flying object by controlling the yaw and pitch angles. The results showed the feasibility of the code in performing the virtual experiments rather than expensive real-world tests.

For future work, it is recommended to test the Artificial Intelligence (AI) control method which based on fuzzy-neural network, to reduce the overshoot and reduce the time of response. It has a quality advantage that made it able to be invested or used normally by aeronautical engineers (in modeling engineering, training and control). In

the last decade, its investment in designing control and guidance systems on the reality has been grown.

REFERENCES

Aksu, A. (2013). Aerodynamic Parameter Estimation of a Missile. *In Metu.*

Belkacem, B., Bachir, N. (2019). *Dynamic Modeling and Control of Large Space Structures : Part I. October.*

Bhagwandin, V. A., Sahu, J. (2012). Numerical prediction of pitch damping derivatives for a finned projectile at angles of attack. *50th AIAa Aerospace Sciences Meeting Including the New Horizons Forum and Aerospace Exposition, January, 1–16.*

Cover, F. (1995). *Review Literature and Arts of the Americas, 1211(July).*

Hang, C. C., Astrom, K. J., Ho, W. K. (1991). Refinements of the Ziegler-Nichols tuning formula. *IEE Proceedings D: Control theory and Applications*, **138(2)**, 111–118.

Kisabo, A. B., Adebimpe, A. F., Okwo, O. C., & Samuel, S. O. (2019). State-Space Modelling of a Rocket for Optimal Control System Design. *Journal of Aircraft and Spacecraft Technology*, **3(1)**, 128–137.

Military handbook. Missile flight simulation. *Part one. Surface-to-air missiles (z-lib.org).pdf. (n.d.).*

Murri, D. G., Jackson, E. B., Shelton, R. O. (2015). *Check-Cases for Verification of 6-Degree-of-Freedom Flight Vehicle Simulations: Volume II: Vol. II (Issue January 2015).*

Oktay, E., Akay, H. U. (2002). CFD predictions of dynamic derivatives for missiles. *40th AIAa Aerospace Sciences Meeting and Exhibit, January.*

R. D. Finck. (1978). *US Air Forces Stability and Control DATCOM. 3200.*

Shelton, A., Martin, C., Silva, W. (2018). Characterizing aerodynamic damping of a supersonic missile with CFD. *AIAa Aerospace Sciences Meeting, 2018, 210059.*

Stalnaker, J. F., Robinson, M. A. (2002). Computation of stability derivatives of spinning missiles using unstructured cartesian meshes. *20th AIAa Applied Aerodynamics Conference, June, 1–7.*

CURRICULUM VITAE (CV)

Name: Kutaibah Srour

Language: Arabic, and English

Education:

- B.S in Aeronautical Engineering CGPa (82 %), Aleppo University
- M.SC in Aeronautical aand Aerospace Engineering CGPa (3.88 out of 4), Gaziantep University.

Conference:

- International Symposium on Aircraft Technology, MRO & Operation, $ISATECH_{21,}$
  hosted by Budapest university of technology & economics,
  Budapest, Hungary between June, 28-30-2021

Work experience:

- Project Manager with Kanaf institution, Syria, Idleb, 2017 – 2018.

  This project aimed to provide education and humanitarian services for children (between 5 and 12 years old)
- Supervisor in Al-Faysal refrigeration factory, Saudi Arabia, 2016.

  Supervised 50 workers to manufacturing refrigerators and freezing devices.